Thermal Loading of Natural Streams

GEOLOGICAL SURVEY PROFESSIONAL PAPER 991

Thermal Loading of Natural Streams

By ALAN P. JACKMAN *and* NOBUHIRO YOTSUKURA

GEOLOGICAL SURVEY PROFESSIONAL PAPER 991

UNITED STATES GOVERNMENT PRINTING OFFICE, WASHINGTON : 1977

UNITED STATES DEPARTMENT OF THE INTERIOR

CECIL D. ANDRUS, *Secretary*

GEOLOGICAL SURVEY

V. E. McKelvey, *Director*

Library of Congress Cataloging in Publication Data

Jackman, Alan P.
Thermal loading of natural streams.

(Geological Survey Professional Paper 991)
Bibliography: p. 38-39.
Supt. of Docs. no.: I 19.16:991
1. Thermal pollution of rivers, lakes, etc. I. Yotsukura, Nobuhiro, joint author. II. Title. III. Series: United States Geological Survey Professional Paper 991.
TD427.H4J3 363.6'1 76-608317

For sale by the Superintendent of Documents, U.S. Government Printing Office
Washington, D.C. 20402
Stock Number 024-001-02959-6

CONTENTS

ILLUSTRATIONS

TABLES

THERMAL LOADING OF NATURAL STREAMS

By ALAN P. JACKMAN and NOBUHIRO YOTSUKURA

ABSTRACT

The impact of thermal loading on the temperature regime of natural streams is investigated by mathematical models, which describe both transport (convection-diffusion) and decay (surface dissipation) of waste heat over 1-hour or shorter time intervals. The models are derived from the principle of conservation of thermal energy for application to one- and two-dimensional spaces.

The basic concept in these models is to separate water temperature into two parts, (1) excess temperature due to thermal loading and (2) natural (ambient) temperature. This separation allows excess temperature to be calculated from the models without incoming radiation data. Natural temperature may either be measured in prototypes or calculated from the model. If use is made of the model, however, incoming radiation is required as input data.

In order to formulate a linear decay model for excess temperature, the equations for back radiation, evaporation, and conduction, derived from the Lake Hefner study of U.S. Geological Survey, are linearized with reference to an arbitrary base temperature. It is shown that the resulting surface dissipation coefficient is predominantly influenced by wind speed and the mass-transfer coefficient of evaporation.

For one-dimensional problems, the transport of excess temperature is solved by the Lagrangian convection model of traveling with an average heated water packet. In two-dimensional problems, a steady-state diffusion model is combined with the one-dimensional decay model. Longitudinal dispersion is neglected in both transport models.

Comparison of observed and calculated temperatures in seven natural streams shows that the models are capable of predicting transient temperature regimes satisfactorily in most cases. Mass-transfer coefficients of evaporation in streams are much higher than those commonly used for long-term calcualtions in a lake. Factors such as ground-water accretion, abrupt changes in thermal loading, and unstable atmospheric conditions are found to have significant impacts on water temperature regimes.

The dissipation of excess heat in natural streams is a gradual process frequently extending over a long downstream distance. For five out of the seven study reaches, the remaining excess heat at a point nearly 30 kilometres downstream was more than 50 percent of the initial thermal load.

INTRODUCTION

The impact of thermal loading (waste heat discharge) on temperature regime of a natural water body is the basic physical information that is required for meaningful assessment of water-quality changes induced by such waste discharges.

The Geological Survey has been engaged for more than 20 years in the study of thermal loading as an outgrowth of the study of evaporational water losses in lakes. The results of the earlier studies have been published in papers by Harbeck (1953), Harbeck, Koberg, and Hughes (1959), Messinger (1963), Harbeck, Meyers, and Hughes (1966), and Harbeck (1970). These studies used the energy-budget equation derived from the Lake Hefner study (Anderson, 1954) and investigated daily- or weekly-average (long-term) thermal regimes of a few western lakes and a couple of natural streams.

Toward the end of 1968, the extension of thermal loading studies to natural streams was deemed urgent in view of the mounting concern about thermal pollution caused by power generation (Parker and Krenkel, 1969). At the same time, keen interest was shown in the collection of synoptic data from thermally loaded streams covering a wide range of meterologic and hydraulic conditions.

Accordingly, the Geological Survey, in cooperation with the Atomic Energy Commission (now the Energy Research and Development Administration), undertook a 1-year program of data collection in six natural streams that were thermally loaded and located in different regions of the country. Briefly, a stream survey consisted of measuring water temperature, meteorologic variables, discharges, and channel geometries at several cross sections downstream from the heat source for a duration of 24 hours. In many streams, two to three surveys were conducted during the year to evaluate seasonal thermal patterns. All survey works were completed between February 1969 and January 1970. In addition, the thermal data of the Susquehana River collected by the Geological Survey in 1962 were considered worthy of reexamination and included in the data set of the present report.

Examination of these stream data revealed that, even though the energy-budget equation adequately describes the heat exchange at the air-water interface, it is not suitable for describing the heat transport. In order to predict natural stream phenomena in terms of hourly (short-term) variations, the equation for conservation of thermal energy must be derived and solved with due considerations given to the transport aspect as shown by recent studies such as Edinger and Geyer (1965), Jaske (1969), Morse (1970), and Harleman (1972) among others.

In solving the thermal energy equation, further-

more, some of the customary models and assumptions had to be reexamined. For example, the steady-state exponential decay law predicts that the excess temperature decreases exponentially with increasing downstream distances. In view of highly variable thermal loading patterns and meteorologic conditions in prototypes, such a simple model could not accommodate short-time or equivalently short-distance phenomena (Jackman and Meyer, 1971). Another example is the equilibrium temperature that is used to calculate the surface heat dissipation coefficient. It is an approximation acceptable only for daily or weekly averages but not for hourly averages (Jobson, 1973a; Yotsukura and others, 1973).

The new approach consists of combining the convective diffusion equation of heat transport with a linearized equation for dissipation of excess heat at the air-water interface (Jackman and Meyer, 1971; Jobson, 1973a; Jobson and Yotsukura, 1973). The approach to surface heat dissipation is Lagrangian in the sense of following average water particles downstream. The dissipation coefficient is calculated with reference to the daily average ambient temperature upstream from the heat source. In addition, a two-dimensional diffusion approach was incorporated into the analysis to facilitate the definition of the mixing zone (Yotsukura, 1972).

The present report describes the final analysis of the thermal data by the analytical models evolved in the last few years and discussed in the above-mentioned papers. The original thermal data and detailed description of field conditions will be presented by a companion paper, which is herein referred to as the Data Report. The following tables describe the measurement units used herein.

ACKNOWLEDGMENTS

The present model study benefited greatly from contributions from a number of specialists in the U.S. Geological Survey. The authors acknowledge, in particular, E. J. Pluhowski, E. F. Hollyday, F. A. Kilpatrick, J. F. Bailey, and R. L. Cory for their valuable contributions throughout the study. The authors also would like to acknowledge cooperations generously given by W. F. Weeks and C. M. Keeler of the Cold Regions Research and Engineering Laboratory, Hanover, N.H., in conducting the thermal study for the North Platte River.

Coordination of the data collection program of this scale was certainly not a simple task. Credit is due E. L. Meyer, whose skill and devotion applied to the task was a major factor in the successful completion of the field work.

EQUATIONS FOR CONSERVATION OF THERMAL ENERGY

Water temperature expresses the thermal energy of

Conversion of units between SI and conventional systems for basic quantities

[This table is based on (1) National Bureau of Standards, 1972, The International System of Units (SI): NBS Special Publication 330. (2) National Physical Laboratory, 1966, Changing to the metric system: H.M.S.O., London. (3) Baumeister, T., 1958, Mechanical Engineers's Handbook: McGraw-Hill Book Co., Inc., New York]

Quantity	*SI units*	*Conventional units*	*Conversion*	
Length	Metre	Foot	1 m = 3.281 ft	1 ft = 0.3048 m
	Kilometre	Mile	1 km = 0.6214 mi	1 mi = 1.609 km
Area	Square metre	Square foot	1 m^2 = 10.76 ft^2	1 ft^2 = 0.09290 m^2
	Square kilometre	Square mile	1 km^2 = 0.3861 mi^2	1 mi^2 = 2.590 km^2
Volume	Cubic metre	Cubic foot	1 m^3 = 35.31 ft^3	1 ft^3 = 0.02832 m^3
Mass	Kilogram	Pound	1 kg = 2.205 lb	1 lb = 0.4536 kg
Force	Newton	Kilogram-force	1 N = 0.1020 kg	1 kg = 9.807 N
		Pound-force	1 N = 0.2248 lb	1 lb = 4.448 N
Energy	Joule	Calorie	1 J = 0.2388 cal	1 cal = 4.187 J
Power	Watt	Calorie per second	1 W = 0.2388 $cal \cdot s^{-1}$	1 $cal \cdot s^{-1}$ = 4.187 W

Conversion of units between SI and conventional systems for derived quantities

[Quantities represent those commonly used in thermal studies and conversions are given at the magnitudes observed under normal climatic conditions]

Quantity	*SI units*	*Conventional units*	*Conversion*
Water density	Kilogram per cubic metre	Pound per cubic foot	1,000 $kg \cdot m^{-3}$ = 62.43 $lb \cdot ft^{-3}$
Wind speed	Metre per sec	Mile per hour	1 $m \cdot sec^{-1}$ = 2.237 $mile \cdot hr^{-1}$
Atmospheric pressure	Newton per square metre	Millibar	10^5 $N \cdot m^{-2}$ = 10^3 mb
Specific heat of water	Joule per kilogram per degree kelvin.	Calorie per gram per degree Celsius.	4,187 $J \cdot kg^{-1} \cdot K^{-1}$ = 1 $cal \cdot g^{-1} \cdot C^{-1}$
Latent heat of vaporization	Joule per kilogram	Calorie per gram	2,495 $\cdot 10^3$ $J \cdot kg^{-1}$ = 596 $cal \cdot g^{-1}$
Radiation and heat flux	Watt per square metre	Calorie per square centimetre per hour.	1,000 $W \cdot m^{-2}$ = 85.97 $cal \cdot cm^{-2} \cdot hr^{-1}$
Mass transfer coefficient of evaporation.	Kilogram per metre per newton.	Gramme per square centimetre per hr per mile-per-hr per millibar.	$2 \cdot 10^{-8}$ $kg \cdot m^{-1} \cdot N^{-1}$ = $3.218 \cdot 10^{-4}$ $g \cdot cm^{-2} \cdot mile^{-1} \cdot mb^{-1}$
Stefan Boltzman constant of black body radiation.	Watt per square metre per (degree kelvin).[4]	Calorie per square centimetre per min per (degree Kelvin).[4]	$5.67 \cdot 10^{-8}$ $W \cdot m^{-2} \cdot K^{-4}$ = $8.14 \cdot 10^{-11}$ $cal \cdot cm^{-2} \cdot min^{-1} \cdot K^{-4}$

a water body. In natural conditions the thermal energy may be considered equivalent to the internal energy. In order to derive an equation for thermal energy balance, one starts with the First Law of Thermodynamics, which says that the increase in total energy content of a body is the sum of all heat inputs to the body minus the amount of work that is performed by the body. When one subtracts from the equation of total energy balance those parts that are related to mechanical energies, namely, kinetic and potential energies, the differential equation for conservation of thermal energy is obtained as (Pai, 1956)

$$\rho C_p \frac{DT}{Dt} = \kappa \nabla^2 T + \Phi + S, \tag{1}$$

where ρ is water density, C_p is the specific heat of water at constant pressure, T is temperature, t is time, κ is the thermal conductivity, Φ is the rate of heat production by viscous dissipation of mechanical energy, and S is the net heat input from sources and sinks.

In equation 1, the operator D/Dt is the substantial derivative, or

$$\frac{D}{Dt} = \frac{\partial}{\partial t} + v_x \frac{\partial}{\partial x} + v_y \frac{\partial}{\partial y} + v_z \frac{\partial}{\partial z}, \tag{2}$$

where v_x, v_y, and v_z are velocities in the respective coordinate directions. The symbol ∇^2 designates the Laplacian operator or a sum of the three second-order partial derivatives with respect to x, y, and z. Equation 1 assumes that water is incompressible even though its density may vary in space and time. Thus, any change in energy content due to volume expansion or compression is neglected. The equation also represents instantaneous balance of thermal energy within an infinitesimal body of water.

Since most applications of the thermal equation in natural water deal with turbulent flows, equation 1 needs to be averaged over a time scale appropriate for a turbulent flow. The procedure, which is based on the Reynolds' classic averaging method (Hinze, 1959), yields the following equation:

$$\frac{DT}{Dt} = \frac{\partial}{\partial x}(k_x \frac{\partial T}{\partial x}) + \frac{\partial}{\partial y}(k_y \frac{\partial T}{\partial y}) + \frac{\partial}{\partial z}(k_z \frac{\partial T}{\partial z}) + \frac{S}{\rho C_p}. \tag{3}$$

Here T represents time-averaged temperature, S represents time-averaged heat sources and sinks, and the symbols k_x, k_y, and k_z are turbulent thermal diffusion coefficients in the respective directions. In comparing equation 3 with equation 1, note that the molecular conduction term, $\kappa \nabla^2 T$, and the viscous dissipation term, Φ, are neglected after averaging, because these are quite small relative to other averaged terms. For example, for every 1-metre drop in the surface elevation of a uniform stream, this much potential energy is converted through viscous dissipation to thermal energy. This is equal to a heat gain of 9.807 joules per kg of water and corresponds to a temperature rise of only 0.0023°C. The turbulent diffusion terms, on the other hand, appear in equation 3 as lump-sum expressions for the correlation that exists between the deviations of instantaneous velocities and temperature from time-averaged values. The symbols v_x, v_y, and v_z in the substantial derivative, D/Dt, are now all time-averaged velocities.

Owing to the three-dimensional nature of equation 3, its solution is often difficult. In order to reduce its dimension, equation 3 may be integrated over the local depth as shown by Leendertse (1970), Prych (1970), and Holley (1971). Assume that the y coordinate is directed vertically upward. By means of Leibnitz's rule of integration and kinematic boundary conditions appropriate for a natural water body, equation 3 is integrated to the following equation:

$$\frac{\partial YT}{\partial t} + \frac{\partial Y v_x T}{\partial x} + \frac{\partial Y v_z T}{\partial z} = \frac{\partial}{\partial x}(YK \frac{\partial T}{x \partial x}) + \frac{\partial}{\partial z}(YK \frac{\partial T}{z \partial z}) + \frac{YS}{\rho C_p} + \frac{H}{\rho C_p} + \frac{H_{bot}}{\rho C_p}. \tag{4}$$

The symbol Y designates local depth, T is depth-averaged temperature, v_x and v_z are depth-averaged velocities, and K_x and K_z are turbulent thermal-dispersion coefficients. The dispersion term in equation 4 consists of two parts. One is the contribution from the correlation between the local deviations of velocities and temperature from depth-averaged values. This correlation is expressed by a gradient-type dispersion term following Taylor's (1954) model in a steady uniform flow. An additive part is contributed by depth averaging of the turbulent diffusion term of equation 3. The source-sink term is now defined by YS where S is the depth-averaged value. The symbol H defines boundary heat influx normal to the water surface and H_{bot} defines one normal to the channel bottom. These terms are introduced into equation 4 by the boundary condition which assumes that incoming heat flux is transported inward by turbulent diffusion without any storage at the boundary.

For a natural stream, where the width is small relative to longitudinal distances, it is often convenient to have one-dimensional thermal equations. Equation 4 may now be integrated over the channel width, using the same techniques as used in deriving equation 4. The result is

$$\frac{\partial AT}{\partial t} + \frac{\partial AVT}{\partial x} = \frac{\partial}{\partial x}(KA \frac{\partial T}{\partial x}) + \frac{AS}{\rho C_p} + \frac{WH}{\rho C_p} + \frac{WH_{bot}}{\rho C_p}. \tag{5}$$

In equation 5, A is the cross-sectional area, T is the

cross-sectional average temperature, V is the cross-sectional average longitudinal velocity, K is the cross-sectional average thermal dispersion coefficient, and S is the cross-sectional average source sink. The symbols H and H_{bot} are width-averaged surface flux and bottom flux, respectively, while W designates the surface width at the cross section.

Even though the details of derivations of the above equations are omitted in the present report, examination of various references shows that these equations are general and most suitable for use in natural water bodies where flows may be transient and boundaries complex. In deriving these equations, no assumptions are made as to the steadiness or uniformity of flow. On the other hand, various diffusion and dispersion terms are added as the averaging progresses from one stage to the next. These terms are introduced as an analogy to gradient-type molecular diffusion. Although some of these diffusive terms have been verified as workable approximations by experiments, notably in a steady uniform flow, one must remember that the expressions for dispersion and diffusion are definitions rather than established physical laws. Fortunately diffusive transport is normally small relative to average-velocity (convective) transport and may even be neglected under certain conditions.

HEAT TRANSFER AT THE AIR-WATER INTERFACE

The mechanics of heat transfer at the flow boundaries of a natural water course is important in thermal loading problems, because the excess thermal energy possessed by water is ultimately dissipated to the air and the soil through such transfers. It is known that heat transfer at the water surface is one of the major factors in determining water temperature under both natural and thermally loaded conditions. In comparison, heat transfer through the streambed is normally small, except possibly in extremely shallow streams flowing over solid beds of rock (Brown, 1972). Moreover, there is very little information currently available on this transfer process. For these reasons, the soil-water interface transfer will be neglected hereafter.

Heat transfer at the air-water interface may be described most conveniently with reference to the one-dimensional thermal equation, because the same surface-transfer equations are applied to the more complex two- and three-dimensional equations. The left side of equation 5 may be simplified by substituting the continuity equation of water. Also the source term, S, and the longitudinal dispersion term, $KA\partial T/\partial x$, are neglected. Equation 5 is then reduced to

$$\frac{\partial T}{\partial t} + V\frac{\partial T}{\partial x} = \frac{H}{\rho C_p Y} . \tag{6}$$

The depth, Y, is defined by A/W according to equation 5.

Four mechanisms have been identified as contributing to the net heat flux, H. They are shortwave radiation, longwave radiation, evaporation, and conduction. The largest of these terms is the shortwave radiation, which may assume values as large as 1,200 watts·m^{-2}. It always contributes a positive component to H since essentially no shortwave radiation is emitted by the water. Incoming shortwave and longwave radiation differ significantly from other components in that they do not depend in any way on water temperature. Moreover, the shortwave radiation has a well-defined dependence on time of day through the sun angle, whereas all other terms, while varying in a somewhat random fashion with time in response to variables such as wind speed, have no deterministic dependence on time.

Outgoing longwave radiation, evaporation, and conduction all depend on the water temperature. Because of the complex nature of some of the dependencies, these terms cause equation 6 to be nonlinear. They do not depend directly on the time, although evaporation and conduction depend on such factors as wind velocity, atmospheric stability, and humidity, which vary with time. The maximum values of these components are considerably smaller than that for incoming shortwave radiation.

The fact that incoming shortwave and longwave radiation do not depend on water temperature enables one to remove these components from the thermal equation through a transformation of the temperature variable. Suppose there was no waste heat discharged into the stream. The temperature, T_n, which would exist under natural conditions is described by the same equation as equation 6 but with H depending on t and T_n, or

$$\frac{\partial T_n}{\partial t} + V\frac{\partial T_n}{\partial x} = \frac{H(T_n,t)}{\rho C_p Y} . \tag{7}$$

It is assumed that the coefficients of equations 6 and 7, such as V and Y, are not affected by thermal conditions. If the excess temperature, T_e, is defined as the difference between T and T_n, then, subtracting equation 7 from equation 6,

$$\frac{\partial T_e}{\partial t} + V\frac{\partial T_e}{\partial x} = \frac{H(T,t) - H(T_n,t)}{\rho C_p Y} . \tag{8}$$

The net flux, $H(T,t)$, may be divided into four components,

$$H(T,t)=H_r(t)-H_b(T)-H_e(T,t)-H_c(T,t), \quad (9)$$

where H_r is the net incoming radiation, both longwave and shortwave, which actually crosses the air-water interface unreflected, H_b is the back radiation (longwave radiation emitted by the water), H_e is the heat flux due to evaporation of water, and H_c is the heat flux due to conduction from the water into the atmosphere. Note that only H_r is independent of T; therefore, if equation 9 is substituted into equation 8, the $H_r(t)$ from the two terms will cancel, and equation 8 is written as

$$\frac{\partial T_e}{\partial t}+V\frac{\partial T_e}{\partial x}= \quad (10)$$

$$\frac{-H_b(T)+H_b(T_n)-H_e(T,t)+H_e(T_n,t)-H_c(\mathrm{T,t})+H_c(T_n,t)}{\rho C_p Y}.$$

This is a considerable simplification, as equation 10 can be solved without knowing the total incoming radiation. Total incoming radiation, in addition to being a large term of considerable variability, is a quantity that is not now being continuously measured and reported by any agency. For each application it must, therefore, be measured, and this requires expensive equipment that is difficult to maintain and calibrate.

In addition to simplifying the modeling problem, excess temperature is a variable of considerable importance in studying the impact of man on the stream environment. In the case of a discharge of waste heat, the heat added to the water will increase the internal energy of the water, thus increasing the water temperature. Thermodynamics dictates that the increase in temperature resulting from a waste discharge is a nearly linear function of the amount of heat added to a unit mass of the water. This increase in temperature is the excess temperature, T_e. Thus, a waste heat discharge may be thought of as a source of excess temperature.

Just as the excess temperature at the point of discharge is a measure of the amount of heat added at that point, the excess temperature at a down-stream point is a measure of the amount of the waste heat that still remains. The solution of equation 10 describes the excess temperature as a function of space and time and, thus, gives an idea of how much of, and to what degree, the stream is affected.

Calculations involving excess temperature are not limited to waste heat discharges. For instance, the recovery of subnormal stream temperatures resulting from cold water releases below impoundments may be estimated using the excess temperature approach. In this case, excess temperatures will be negative owing to the fact that the stream has lower energy content than it would under natural conditions.

In order to calculate the excess temperature using equation 10 it will be necessary to know T_e at some point as a function of time, for example, a boundary condition. This may be specified at the point of discharge, in the case of a waste heat discharge, by dividing the rate of discharge of waste heat by the product of the density, the specific heat, and the volumetric rate of flow of waste water into the stream. It is also possible, in those cases where the stream mixes rapidly, to measure the difference between the temperature at a point just upstream of the discharge point and the temperature of the stream once fully mixed below the discharge point. Both of these approaches assume that the temperature just upstream of the discharge is the natural temperature. If this is not the case, it will be necessary to estimate the natural temperature at the upstream point.

The solution of equation 10 for excess temperature requires expressions for the heat exchange due to outgoing longwave radiation, evaporation, and conduction. In the case of evaporation and conduction mechanisms, there are a number of expressions available. Much room for improvement in these expressions exists. The models discussed here are among the most frequently used.

The longwave or "thermal" radiation emitted by a body is known to be related to the temperature of a body by the Stefan-Boltzmann equation:

$$H_b=\sigma\epsilon(T+273.16)^4, \quad (11)$$

where $\sigma=5.67\cdot10^{-8}$ watts $\cdot m^{-2}\cdot{}^\circ K^{-4}$ is the Stefan-Boltzmann constant, ϵ is the total hemispherical emissivity, T is temperature of the body in degrees Celsius, and H_b is given in units of watts $\cdot m^{-2}$. Anderson (1954) reported that for natural waters the emissivity is essentially independent of the dissolved-solid concentration and temperature. Emissivity was also found to be independent of the suspended sediment load, but an oil layer on the water surface significantly reduces emissivity. Anderson concluded that for oil-free natural waters the emissivity is 0.970 ± 0.005.

In spite of extremely precise formulation provided by equation 11, there are still inaccuracies that may attend its use with natural water bodies. These errors arise because of errors in the temperature. Most longwave radiation emitted by a water surface is produced in the first 100 μm below the water surface (McAlister and McLeish, 1969). Ewing and McAlister (1960) found that the temperatures within this layer

may differ significantly from that temperature which would be measured with the smallest conventional temperature measuring device placed as close to the water surface as possible. The true surface temperature is generally found to be lower than the bulk water temperature. Thus, calculations of back radiation based on bulk temperature will overestimate the actual back radiation. The error in calculated back radiation will usually be less than 3 percent, because the surface is usually less than 2°C (Celsius) cooler than the bulk. Equation 11, with the temperature measured near the surface using conventional thermometry, should give a satisfactory estimate of back radiation for most purposes.

Evaporation contributes to the heat flux at the air-water interface in two ways. First, in order for water in the liquid state to enter the gaseous state an amount of energy, the latent heat of vaporization must be added. This energy, approximately $2.5 \cdot 10^6$ joules per kg of water, must be supplied from the water body. Thus, the water body loses energy by the evaporation process. In addition, some mass of water is lost, and this represents a decrease in the total energy of the system. This term does not have any effect on the energy content per unit mass and becomes important only in cases where a change in the mass of the system is significant. It will be ignored in this work.

The rate of evaporation from a water surface is related to the rate at which water vapor may be transferred away from the interface. The transport process involved is a turbulent diffusion process. If the air far away from the interface has a lower partial pressure of water vapor than the air very near the interface, then a gradient for diffusion will exist. Note that this gradient may be reversed and condensation may occur, causing an influx of energy to the water body. The partial pressure of water vapor at the interface is the saturation vapor pressure for water at the temperature of the interface that will be approximated by the bulk water temperature.

The diffusive flux of water vapor away from the interface may be expressed as

$$E = \frac{1}{RT_2} k_{H_2O} \frac{\partial p_{H_2O}}{\partial y}, \tag{12}$$

where R is the gas constant, T_2 is the air temperature, k_{H_2O} is the turbulent diffusivity of water vapor in air, and p_{H_2O} is the vapor pressure. The diffusivity is known to be a function of wind velocity. If the wind velocity profile follows a logarithmic form, it may be shown (Priestly, 1959) that at a given distance, y_2, above the surface

$$k_{H_2O}(y_2) = \frac{\kappa^2 v_2}{\eta \, y_2 \ln(y_2/y_0)}, \tag{13}$$

where κ is the von Karman constant taken to be 0.40, η is the turbulent Schmidt number, v_2 is the wind speed at elevation y_2, and y_0 is a constant known as the roughness. This expression is valid only during periods of neutral atmospheric stability, but it shows a direct proportionality of k_{H_2O} on wind speed.

Among many existing models of evaporation, the most commonly used are the mass transfer models, which are also called Dalton-type equations. These models recognize that evaporation is proportional to the vapor pressure difference and that the coefficient of proportionality is a function of wind speed. Marciano and Harbeck (1954) and Harbeck (1962) studied them carefully and found that the following simple formula gives adequate results for lakes and reservoirs when all quantities are time averaged over a period of 1 day or longer:

$$E = N v_2 (p_s - p_2), \tag{14}$$

where N is the mass transfer coefficient, v^2 is the wind speed at some elevation (usually two metres), p_s is the saturation vapor pressure of water at the temperature of the surface, and p_2 is the partial pressure of water vapor at the same elevation as used for wind speed.

Harbeck (1962) found that the value of N varies with the surface area of a water body according to

$$N = 3.42 \cdot 10^{-8} \cdot A_s^{-0.05}, \tag{15}$$

where A_s is the surface area in square meters and N is given in units of $kg \cdot m^{-1} \cdot newton^{-1}$. Taking a typical stream to have an effective surface area for evaporation of 1,000 m^2, one finds a value of $N = 2.42 \cdot 10^{-8}$ $kg \cdot m^{-1} \cdot newton^{-1}$.

It has been recognized for some time that the value of N may not be a constant but may depend on wind direction and atmospheric stability. While these factors may not be important when using data averaged over long periods of time, they may be very important when using hourly data. Brutsaert and Yeh (1970) showed that rather than N depending on the area of a water body, it should depend on fetch. They find that N should be proportional to the fetch to the -0.25 power. The average fetch length will depend on wind direction for all but circular bodies, and it is very difficult to assess this factor for streams.

There is an increasing interest in the effect of atmospheric stability on the mass transfer process. It is generally believed that under unstable atmospheric conditions the rate of mass transfer will be increased owing to the existence of buoyancy-driven natural convection currents. And under stable conditions, the value of the eddy diffusivity will be reduced, reducing the rate of mass transfer. On the basis of the Lake

Mead studies, Harbeck, Kohler, Koberg, and others (1958) recommended a stability dependent form for the mass transfer coefficient:

$$N=1.04\cdot 10^{-8}\left[1-0.03(T_2-T)\right], \tag{16}$$

where T is surface water temperature in °C, T_2 is the air temperature in °C, and N is given in units of $kg\cdot m^{-1}\cdot newton^{-1}$.

The evaporative heat flux may be calculated directly from the flux of water vapor, E, using any of the above expressions. This is done by multiplying the flux by the latent heat of vaporization, λ, so that

$$H_e=\lambda E. \tag{17}$$

A commonly used value of λ is $2495\cdot 10^3$ joules per kg.

The conductive heat flux has generally been calculated from the evaporative heat flux, as was first suggested by Bowen (1926). It may be shown that if the vertical fluxes of water vapor and heat are independent of distance from the surface, and if the turbulent diffusivities of heat and mass are identical, then

$$H_c=B\,H_e \text{ and} \tag{18}$$

$$B=6.1\cdot 10^{-4}\cdot P(T-T_2)(p_s-p_2)^{-1}, \tag{19}$$

where B is the Bowen Ratio and P is the atmospheric pressure in newtons m^{-2}. Temperatures are in degrees Celsius, and vapor pressures are expressed in $newtons\cdot m^{-2}$.

Equations 11, 17, and 18, in conjunction with equations 14 and 19, describe all the fluxes appearing in the one-dimensional excess temperature model, equation 10. The same fluxes are also needed for the two-dimensional excess temperature model.

The one-dimensional excess temperature equation can now be solved, provided that necessary initial and boundary conditions are specified and that the wind speed and partial pressure of water vapor at the 2-m level are known. Unfortunately, all the flux terms except the conductive flux, H_c, are nonlinear functions of water temperature, T. The back radiation depends on the fourth power of water temperature according to equation 11. The evaporative flux depends on the saturation vapor pressure of water, which is an exponential function of water temperature,

$$p_s=610\cdot\exp\left[19.7071-5383.2\cdot(T+273.16)^{-1}\right] \tag{20}$$

where p_s has units of $newtons\cdot m^{-2}$ and T is in degrees Celsius.

Linearized approximation of H_b and H_e may be obtained by expanding equations 11 and 17 as Taylor series about an arbitrary base temperature, T_b, and truncating all terms of second order and higher. Subtracting the expressions for T_n from those for T, the following equations are obtained:

$$H_b(T) = H_b(T_n) + 4\sigma\epsilon(T_b + 273.16)^3\cdot T_e, \tag{21}$$

$$H_e(T) = H_e(T_n) + 5383.2\cdot\lambda N v_2 p_s(T_b)\,(T_b + 273.16)^{-2}\cdot T_e, \text{ and} \tag{22}$$

$$H_c(T) = H_c(T_n) + 6.1\cdot 10^{-4}\cdot P\lambda N v_2 T_e\,. \tag{23}$$

Substituting equations 21, 22, and 23 into equation 10, the one-dimensional excess temperature equation is

$$\frac{\partial T_e}{\partial t}+V\frac{\partial T_e}{\partial x}=-\frac{UT_e}{\rho C_p Y}, \tag{24}$$

where U, defined as the heat dissipation coefficient, closely resembles the conventional engineering heat transfer coefficient and is given by

$$U = 4\sigma\epsilon(T_b+273.16)^3 + \lambda N v_2\left[5383.2\cdot p_s(T_b)\,(T_b+273.16)^{-2} + 6.1\cdot 10^{-4}\cdot P\right]. \tag{25}$$

For most computations, a constant temperature may be used as T_b so long as it does not deviate excessively from natural temperature T_n (Jobson, 1973a, Yotsukura and others, 1973). Two other coefficients for surface heat dissipation may be defined in conjunction with U. These are

$$U_*=\frac{U}{\rho C_p} \text{ and} \tag{26}$$

$$\tau_d=\frac{\rho C_p Y}{U}\,. \tag{27}$$

In solving equation 24, note that the left side is identical to the one-dimensional substantial derivative, DT_e/Dt. By definition, it describes the time variation of T_e of a particular water packet. Equation 24 can be simplified by interpreting it in the Lagrangian sense of following the water packet moving with velocity V. The travel time, τ, may be defined such that

$$x = \int_0^\tau V d\tau' + x_0 \tag{28}$$

and

$$t = \tau + t_0, \tag{29}$$

where x_0 and t_0 are given values of x and t at $\tau=0$. Equation 24 is, thus, reduced to an ordinary differential equation with τ as the single independent variable:

$$\frac{dT_e}{d\tau} = -\frac{T_e}{\tau_d}. \tag{30}$$

The analytical solution to this equation is easily obtained as

$$T_e = T_{eo} \exp\left(-\int_0^{\tau} \frac{1}{\tau_d}\, d\tau'\right), \tag{31}$$

where T_{eo} is an initial excess temperature at $\tau=0$.

Note that the time constant, τ_d, depends on U, which, in turn, depends on v_2 and T_b as shown in equation 25. Even if T_b may be assumed constant, v_2, the 2-m wind speed, varies rapidly with time. Thus, τ_d is a function of time. It is often desirable to predict downstream temperature for a travel time longer than the interval for meteorological observation; for example, employ equation 31 for a travel time of 24 hours using wind-speed data collected at hourly intervals. In cases such as this, the travel time must be segmented into periods, $\Delta\tau$, equal in length to the period for a wind speed observation, and the integral in the exponential term of equation 31 becomes a summation of $\Delta\tau/\tau_d$ over the travel time τ. This segmentation causes the calculations to have a serial character much as would a direct numerical integration of equation 10, although less tedious and free of convergence problems. Yotsukura, Jackman, and Faust (1973) have shown that the linearization results in appreciable errors when the excess temperature is larger than 10°C. In such cases the numerical integration of equation 10 would be an attractive alternative.

Recapitulating on the various heat exchange equations introduced in this section, it is evident that the description of evaporation processes needs further improvement. Equation 14 was adopted in this report on the basis of proven practical usefulness, but it is an empirical equation. It will be very attractive to develop equations that do not depend on water temperature. The aerodynamic models of estimating evaporation have an advantage over the mass transfer models in that they do not contain empirical coefficients such as the mass transfer coefficient and that they accommodate more theoretically sound description of evaporation processes. Jobson (1973b) and Pierson and Jackman (1975) reported progress made in this course of approach.

The total incoming radiation, H_r, was removed from the energy equation when equation 10 was derived for excess temperature. This heat flux is important when the natural temperature needs to be estimated. This quantity is best determined experimentally. When experimental determination is not possible, however, there are models for both the longwave and shortwave incoming radiation. Sellers (1965) described a number of models for both fluxes. Koberg (1964) presented a method for estimating longwave radiation, and Anderson (1954) presented a model for determining the reflectivity of a natural water surface. These models should only be employed where direct measurement of incoming radiation is not feasible.

It is also worth noting that, in spite of nonlinear relations between heat fluxes and water temperature, the heat exchange equations and their linearized approximations can be used for widely varied time intervals ranging from 15 minutes to more than 24 hours, on the condition that they are used within a natural range of temperature variability (Jobson, 1972; Yotsukura and others, 1973).

ANALYSIS OF NATURAL TEMPERATURE

As was demonstrated above, the use of excess temperature, T_e, is a very attractive method of evaluating man's impact on the thermal regime of a stream. This technique may be used where excess temperature is the only variable of interest, as might be the case in many planning studies. There will, however, always be instances where one must predict actual water temperatures. A study of the influence of discharges on the biota of a stream is one example. Another example is where multiple manmade alterations of unknown magnitude affect the thermal regime of a stream in a given reach. In such cases, the excess temperature alone is not enough. It will also be necessary to determine the natural temperature. In general it is not possible to observe T_n downstream of a waste heat discharge, since that discharge will have modified the natural temperature. An exception to this occurs when excess heat mixes slowly in the transverse direction, allowing unmodified natural temperature on one side of the stream throughout the reach. Here the natural temperature may be observed. Where this is not possible, the natural temperature must be predicted.

In the analysis of natural temperature, a linearization of surface heat flux term, $H(T_n,t)$, may not offer much advantage, because the incoming radiation, H_r, cannot be removed from the equation for T_n as was the case for T_e. In solving equation 7, therefore, all four components of H must be taken into consideration.

It is also clear that the variation of depth, Y, is of comparable importance to the right side of equation 7 as that of H. Natural streams frequently have significant depth variations in both longitudinal and transverse directions. It is common to think of the stream as made up of an assemblage of shallow, fast-flowing riffles separating deep, slow-flowing pools. Pool and

riffle regimes are frequently encountered in nature. This casts considerable doubt on any assumption of depth uniformity in either longitudinal or transverse direction. Some insight to the effect of longitudinal depth variation on the natural temperature may be gained by resorting to the concept of the thermally homogeneous stream.

THERMALLY HOMOGENEOUS STREAMS

A thermally homogeneous stream is defined as one for which no longitudinal gradient of temperature exists. The temperature is thus a function of time but not of position. Parts of shallow streams far downstream of their headwaters may approach homogeneity rather closely. Consider a steady uniform stream where V and Y are constants denoted as V_o and Y_o and where a sinusoidal net heat flux is assumed as follows:

$$H(T_n,t) = H_o \cos \omega t. \tag{32}$$

Substituting equation 32 into equation 7, the thermal equation is

$$\frac{\partial T_n}{\partial t} + V_o \frac{\partial T_n}{\partial x} = \frac{H_o}{\rho C_p Y_o} \cos \omega t. \tag{33}$$

If the stream is thermally homogeneous, then, by definition, $\partial T_n/\partial x = 0$ and equation 33 can be integrated to

$$T_n = T_{no} + \frac{H_o}{\rho C_p Y_o \omega} \sin \omega t, \tag{34}$$

where T_{no} is the temperature at $t=0$. As there are no longitudinal gradients of temperature, equation 34 is valid throughout the homogeneous portions of the stream.

Now assume that this homogeneous water suddenly enters a reach where the depth changes to $Y = aY_o$. If a is constant, Y and V are constant. The surface heat flux along the new reach is assumed the same as before. The thermal balance in the new channel is thus

$$\frac{\partial T_n}{\partial t} + V \frac{\partial T_n}{\partial x} = \frac{H_o}{a\rho C_p Y_o} \cos \omega t. \tag{35}$$

The boundary condition at the entrance to the new reach is given by equation 34.

Equation 35 can be integrated by the introduction of travel time, τ, as defined by equations 28 and 29 in the previous section. The solution that satisfies the boundary condition is obtained as

$$T_n(t,\tau) = T_{no} + \frac{H_o}{\rho C_p Y_o \omega} \sin \omega(t-\tau) + \frac{H_o}{a\rho C_p Y_o \omega} [\sin \omega t - \sin \omega(t-\tau)]. \tag{36}$$

Equation 36 may be interpreted in two different ways. The travel time, τ, is equal to x/V, where x is the downstream distance measured from the entrance to the new channel. Thus, by fixing a value for τ, equation 36 gives temporal variation of water temperature observed at a fixed point. Alternatively, by fixing a value for t, equation 36 gives an instantaneous temperature profile along the channel. The first method of interpretation is used here.

Figures 1 and 2 show temporal variations of temperature, $T_n(t) - T_{no}$, as observed at several positions, which are expressed in units of traveltime rather than distance. Note that the reference temperature, T_{no}, is constant but arbitrary. Figure 1 is for doubling the depth ($a=2$), and figure 2 is for halving the depth ($a=\frac{1}{2}$). The value of ω is $\pi/12$ radians per hour, and $H_o/\rho C_p Y_o \omega$ is assumed to be unity. In both figures it is clear that the temperature regime in the new channel became nonhomogeneous, as temperature at a given time depends on position. In other words, longitudinal temperature gradients were introduced to the new channel as the result of depth change. According to figure 1, at a position 12 hours downstream of the point at which the depth of the channel is doubled, temperature is constant. Amplitude of the diurnal oscillation decreases continuously as a position approaches the 12 hour point from either direction. This is a somewhat pathological condition that occurs only for a doubling of depth.

Figure 1 demonstrates that when the depth increases, the downstream diurnal amplitude will be less than that for the homogeneous stream. On the other hand, when the depth decreases, downstream diurnal amplitudes will be greater than that for the homogeneous stream, as seen in figure 2. Another interesting effect of the depth change is the shift of the time for maximum and minimum temperatures. For instance, while the temperature in the homogeneous stream reaches a maximum at 30 hours, the maximum temperature will occur at about 28 hours for a point 3.3 hours downstream and about 32 hours at a point 20.7 hours downstream, in the case of halving of depth. When $a=1$, equation 36 reverts to equation 34, and there is no longitudinal temperature gradient at any location.

These results, although highly idealized, suggest some conditions one would expect to find in a natural stream. For a thermally homogeneous regime, the amplitude of the diurnal temperature oscillation should be the same for all positions. Further, the time at which the maximum and minimum temperatures are observed should be the same for all positions. On the other hand, there are a number of factors that could prevent even a very shallow natural stream from

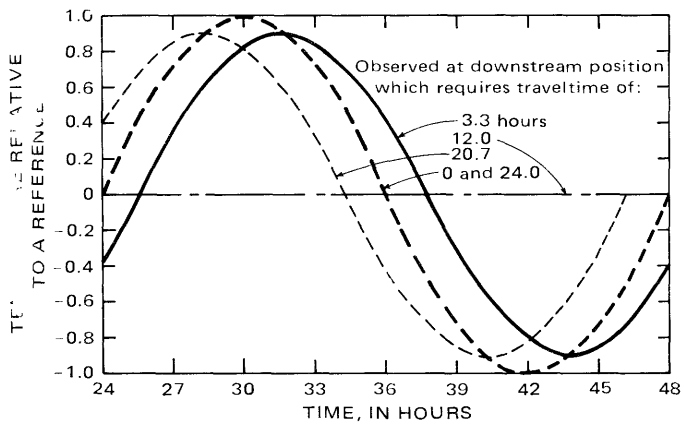

FIGURE 1.—Temporal variations of water temperature at five positions in a hypothetical channel with doubled depth ($a=$).

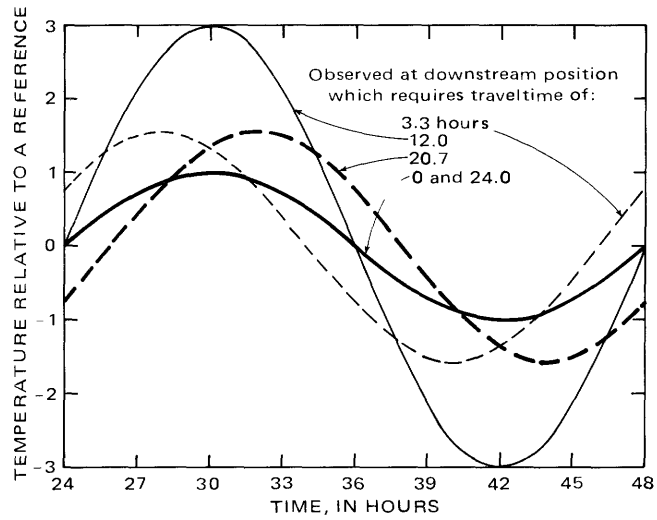

FIGURE 2.—Temporal variations of water temperature at five positions in a hypothetical channel with halved depth ($a=½$).

becoming thermally homogeneous. Longitudinal variations in depth can prevent homogeneity in a channel of any size. However, these variations will have an effect only if the depth variations are such that the average depth (averaged with respect to longitudinal position) changes over relatively long distances. A particle of water passing through a short, shallow reach will suffer a more rapid temperature increase at midday than would a particle of water of average depth. But owing to shortness of the shallow reach, the actual difference in temperature between the two particles may be quite small, assuming they were initially at the same temperature, and this difference would be eliminated if the shallow reach was followed by a short, deep reach.

Variations in the exposure of a stream to incoming radiation or wind can also prevent a stream's attaining thermal homogeneity. Passage through a deep, narrow canyon will significantly reduce the total radiation incident on the water surface during a day. In such a case, a longitudinal gradient in temperature can be established even if the stream was homogeneous and free of such gradients at the upstream end of the canyon. Passage through a reach with appreciably different exposure to wind would produce a similar effect. Both radiation and wind exposure are affected by bankside vegetation (Pluhowski, 1970).

THERMAL HOMOGENEITY OF THE POTOMAC RIVER

Very little data on thermal homogeneity of streams exist. The addition of waste heat to a stream induces longitudinal temperature gradients. This renders an otherwise homogeneous stream nonhomogeneous. Thus, it is impossible to determine whether the streams studied here were or were not homogeneous, and this study adds little to what is known about this concept. The data on the Potomac River are a notable exception. Two of the three studies at this site were conducted under conditions such that the heated plume, which discharged at the left bank, did not affect the water near the right bank for at least 35 km downstream of the discharge site. The Potomac is 500–1,000 m wide in this reach and 1–2 m deep. The shallow nature of the stream led to greatly inhibited lateral mixing. The third study was at an extremely low river discharge, and the large fraction of river water that was diverted through the powerplant condensers was able to reach the right bank within about 3 km of the discharge point.

Figure 3 shows a map of the Potomac study reach and a plot of average depth as determined by discharge measurements versus the longitudinal position along this reach. It reveals considerable variability in depth. The pool at the end of the reach is the result of backwater behind the lip of Great Falls natural dam. The pool at about 8 km is utilized for ferry crossings. The shallow area below the power plant site will not permit operation of small outboard motors during very low flows.

During both the March and May studies in 1969, a helicopter equipped with a Barnes PRT–5 radiometer was employed to determine longitudinal and transverse temperature patterns in the river. Figure 4 presents data from the overflight of several different cross-sections during the March study. Note that even as far downstream as section 11, 35 km from the powerplant, the heat plume is still confined essentially to the left half channel. These temperature determinations were all made within a 30-minute period starting at 12:05 p.m. on March 11, 1969.

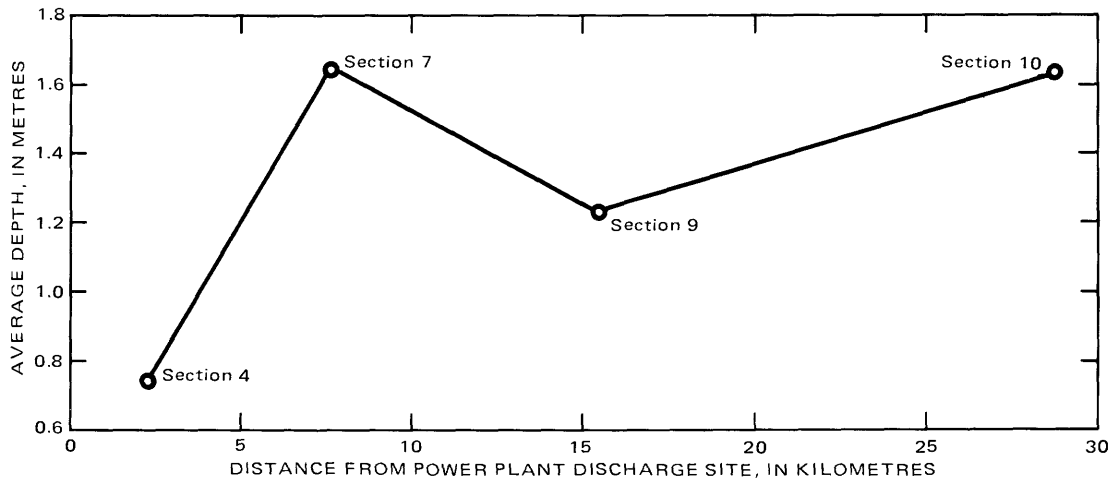

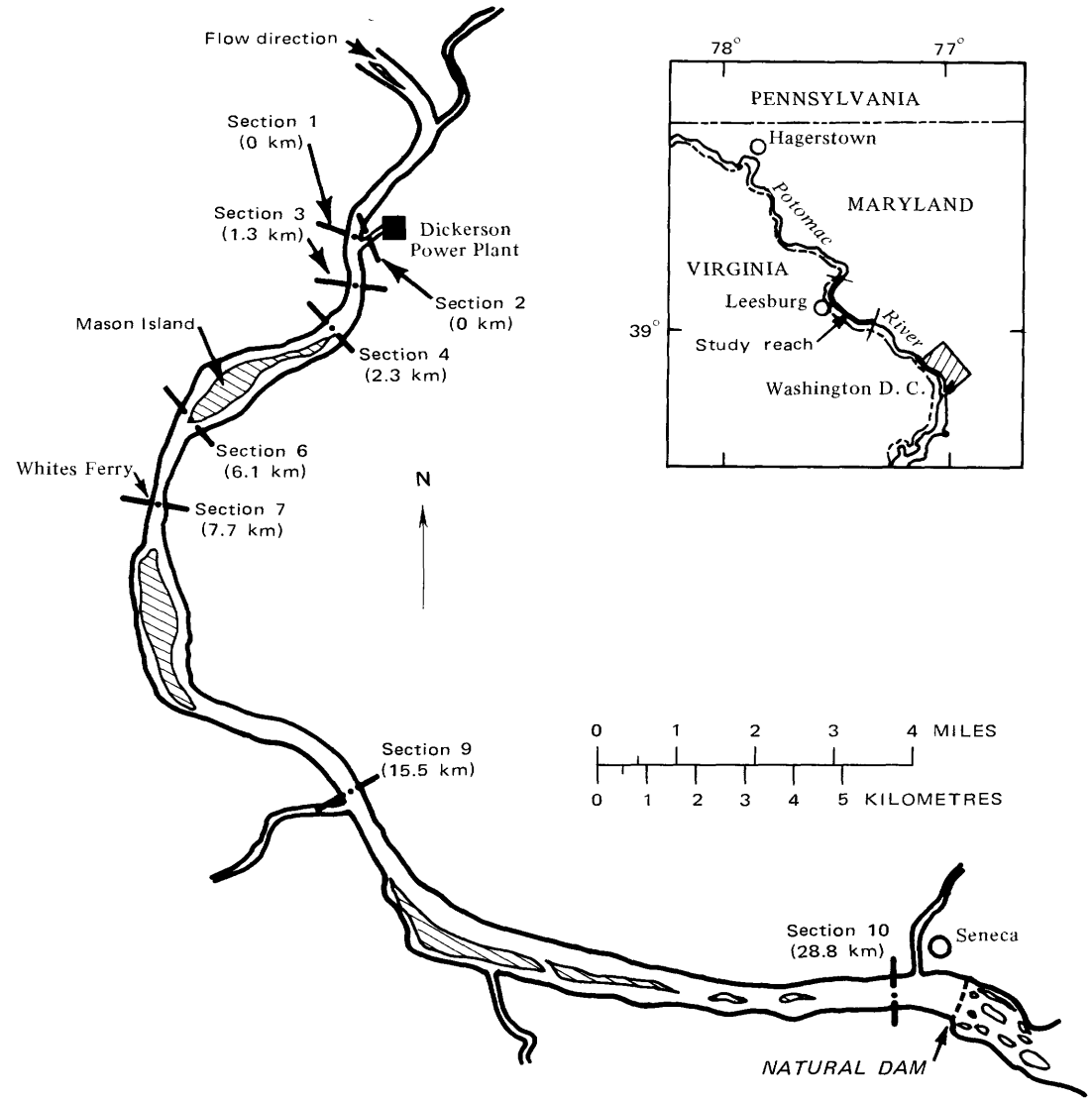

FIGURE 3.—Sketch of the Potomac River study reach below Dickerson Power Plant, Maryland.

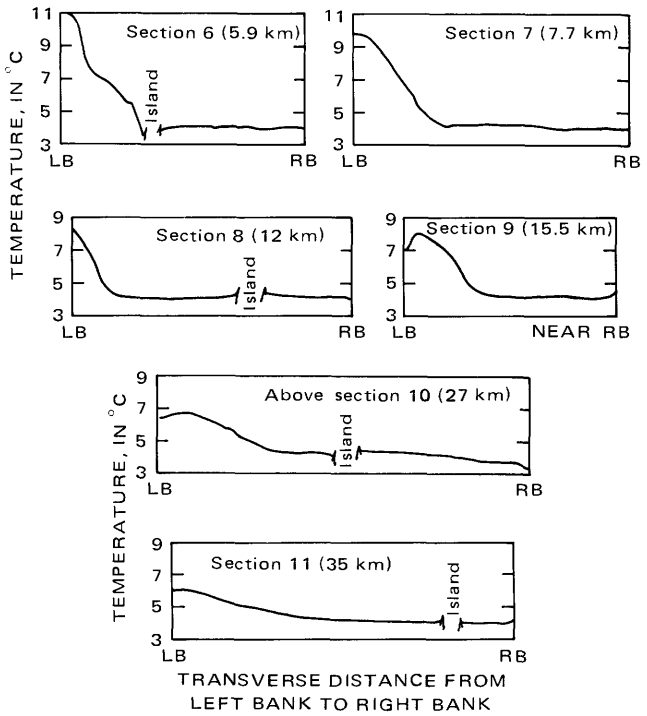

FIGURE 4.—Transverse profiles of water temperature at selected sections, the Potomac River below Dickerson Power Plant, Maryland, March 11, 1969.

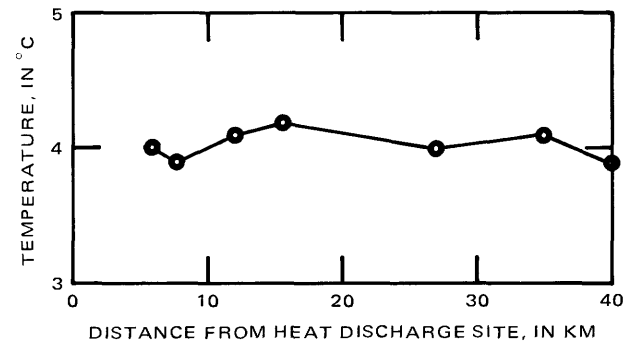

FIGURE 5.—Longitudinal profile of natural water temperature near right bank, the Potomac River below Dickerson Power Plant, Maryland, March 11, 1969.

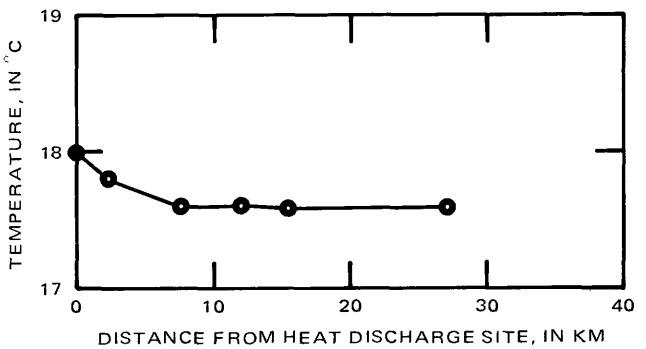

FIGURE 6.—Longitudinal profile of natural water temperature near right bank, the Potomac River below Dickerson Power Plant, Maryland, May 14, 1969.

Careful comparisons of the radiometer measurements with simultaneous ground measurements made using Whitney thermometers show agreement to within 0.1°C, except in the hottest part of the plume where appreciable "cold skin" effect is observed. This effect is caused by the evaporation and conduction at the water surface. There is a thin film of water at the surface where transport of heat is solely by molecular conduction, because turbulent transport diminishes as one approaches the water surface from below. As the heat loss is occurring at the upper edge of this film, and the heat must be supplied from below the film, a net flux of heat toward the surface results in the temperature at the surface being somewhat lower than the temperature below the film. Ewing and McAlister (1960) have shown that this film will not be penetrated by turbulence even in the presence of waves unless the waves are breaking.

The water temperature near the right bank apparently was unaffected by the thermal discharge throughout the reach, and the temperatures observed with the airborne radiometer are, to within the limits of accuracy of our observations, identical to those measured on the ground.

Figures 5 and 6 show the radiometer observations of natural temperature as a function of longitudinal position for the March and May studies, respectively. In both cases the natural temperature is nearly constant with position. The maximum variability is 0.4°.C. There does appear to have been a cooling trend in the upper part of the reach during the May study, but this is probably not significant.

On the basis of figures 5 and 6, it seems reasonable to conclude that the Potomac River near Dickerson, Maryland, is an example of a thermally homogeneous stream. In spite of some known variations in depth, there is no distance-averaged longitudinal gradient of natural temperature, and local gradients are small.

Figure 4 reveals that there were some observable transverse gradients in natural temperature, particularly at section 10. However, the greatest lateral fluctuation of natural temperature was at section 1, just above the thermal discharge site. Figure 7 shows natural temperature versus transverse position at section 1, observed at several times during the March study. At some times the lateral variations in temperature were quite pronounced.

It is difficult to ascertain the source of these variations. Monocacy River joins the Potomac River on the left bank about 2.5 km upstream of the site. The flow of the river was small, about 20 m^3 sec^{-1} compared to 149

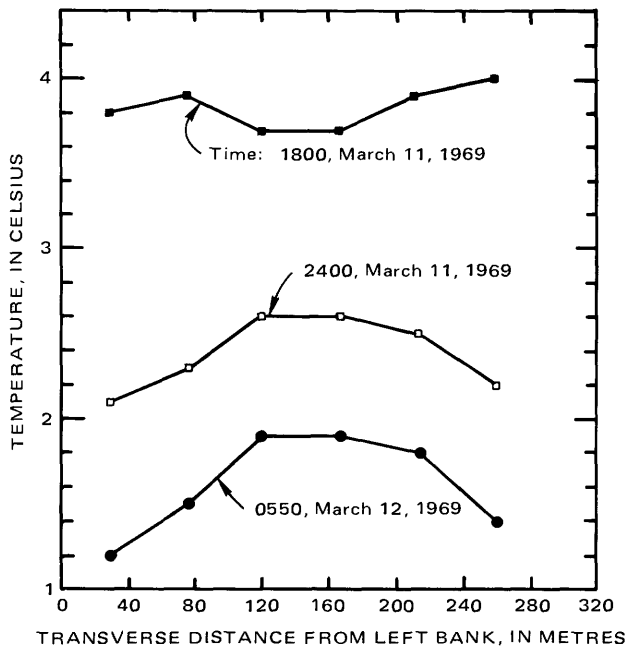

FIGURE 7.—Transverse profile of natural water temperature at section 1, the Potomac River above Dickerson Power Plant, Maryland, March 11–12, 1969.

m^3sec^{-1} for the Potomac, and the variations do not appear to be substantially related to this inflow. The South Branch of the Potomac River joins at the right bank about 30 km upstream. This is a large flow and the slow transverse mixing could lead to variations, but again the pattern of the variations does not seem to support the idea that variations were caused by unmixed inflow. Judging from the pattern of cool centerstream conditions during the day and warm centerstream conditions during the night, it seems most probable that there is a long, deep channel in the center of the stream upstream of section 1. The airborne radiometer results indicate, however, that transverse variations of temperature are less pronounced at most downstream sections.

PREDICTION OF NATURAL TEMPERATURE

When one assumes a thermally homogeneous stream, the longitudinal gradient term, $\partial T_n/\partial x$, vanishes, and equation 7 is reduced to

$$\frac{dT_n}{dt} = \frac{H}{\rho C_p Y}. \tag{37}$$

An explicit finite difference form to solve equation 37 numerically is

$$T_n(t+\Delta t) = T_n(t) + \frac{H(T_n(t), t+\frac{\Delta t}{2})\cdot \Delta t}{\rho C_p Y} \tag{38}$$

Note that H for an interval Δt is calculated by using known water temperature, T_n, at t and given meteorologic conditions at $t + \Delta t/2$.

Figures 8 and 9 are the results of calculations using equation 38 for the station nearest the right bank of the left channel at section 4 of the Potomac River. As the initial condition, the temperature observed at this station during the first measurement of the study was used. The heat-flux term was adjusted by trying various combinations of the depth, Y, and the mass transfer coefficient, N, in order to investigate an optimum

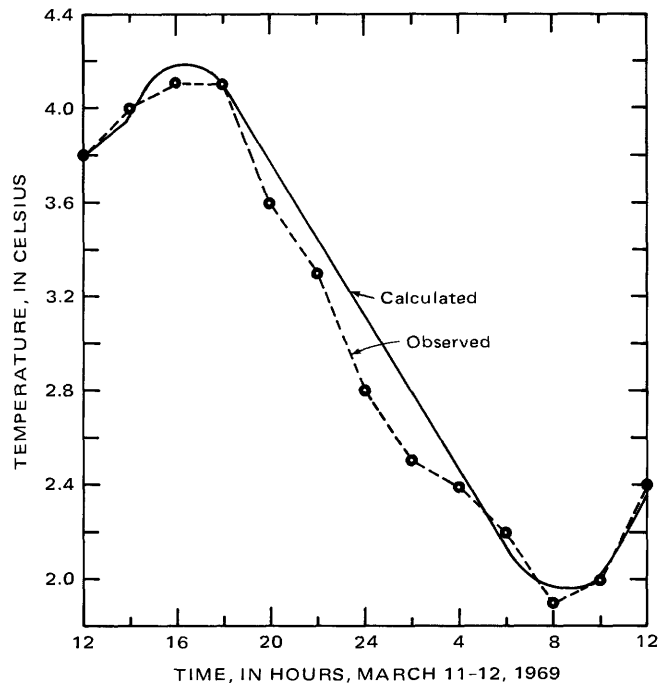

FIGURE 8.—Comparison of observed and calculated natural water temperatures at section 4, the Potomac River below Dickerson Power Plant, Maryland, March 1969.

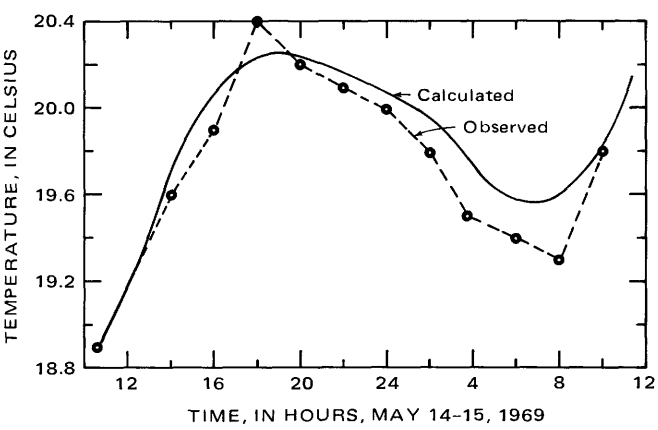

FIGURE 9.—Comparison of observed and calculated natural water temperatures at section 4, the Potomac River below Dickerson Power Plant, Maryland, May 1969.

range of N values suitable to stream conditions. The adjustment of parameters was done in steps to improve the fit of calculated temperature at the end of a run with the observed temperature at that time. Based on data from the March study, the best combination was found to be $Y=1.83$ m and $N=2.31\cdot10^{-8}$ kg·m^{-1}·newton^{-1}. This depth value is somewhat disturbing, since all observations of depth above section 4 would suggest a value near, and perhaps slightly less than, 1 m. This error could be due to consistently high radiometer readings, but in this case we would expect poor prediction during the night when solar radiation was near zero. This is not the case, and the cause of this depth discrepancy remains an unanswered question. It should be noted that 1.83 m is, however, fairly typical of the depth in much of the rest of the river.

The calculated temperature at section 4 for the March study is presented as a function of time in figure 8. The calculated values agree quite well with the observed values. The maximum discrepancy is 0.3°C, and the average of the absolute error over the 24-hour period is about 0.1°C. The shape of the calculated curve is somewhat sensitive to the value of the mass transfer coefficient, N.

Data from the May study on the Potomac was analyzed using the same procedure. However, both Y and N were fixed at values found for the March data. The results are presented in figure 9. The agreement is again very good. A maximum error of 0.3°C and an average absolute error of about 0.2°C is observed. Note that, because depth was already established by the March study, there is no requirement that calculated and observed temperatures agree at the end of the 24 hour period.

The second method of calculating natural temperature is to solve equation 7 directly without assuming the state of thermal homogeneity. By introducing the travel time τ, as the single variable, equation 7 is reduced to an ordinary differential equation. For a uniform subreach, an explicit difference scheme for the differential equation is

$$T_n(\tau+\Delta\tau) = T_n(\tau) + \frac{H(T_n(\tau),t_o+\tau+\frac{\Delta\tau}{2})\cdot\Delta\tau}{\rho C_p Y} \cdot \qquad (39)$$

Equation 39 was applied to the data from the Potomac River. As explained previously, equation 39 is a Lagrangian equation of temperature for a packet of moving water. In order to compare calculated temperatures with observed ones at a fixed location, equation 39 was solved repeatedly for different t_o and T_{no} (t_o) observed at section 1. The value of $\Delta\tau$ was chosen to be 1 hour. As the observed depth was used in equation 39, the value of N was smaller than that found in the homogeneous stream calculations. It was fixed at $N=1.5\cdot10^{-8}$ kg·m·$^{-1}$ newton^{-1} for the March and May data.

Some results of this calculation are shown in figure 10. The agreement with observed temperature is generally satisfactory except at section 7 for the March study, where the calculation underestimates the observation by almost 1°C. The observation station, number 9 of section 7, was located at the midstream in the March study, and about 45 percent of the total discharge was flowing to the left side of this station. It was first suspected that there may have been some effects of the heated plume. However, the air-borne radiometer data indicated that this station was clearly outside the heated plume. A more reasonable explanation appears to be the variation of T_{no} at section 1. Between 0150 and 0550 hours, March 12, water temperature near the left bank, which was used for the calculation, was cooler than the midstream by 0.7 to 0.9°C. This initial difference could have been convected downstream without much modification. The water near the left bank side at section 7 could actually have been cooler than midstream for the period between 0720 and 1120 hours, March 12. For the May study, the transverse variation of T_{no} (t_0) between the left bank and midstream was between 0.1 to 0.4°C throughout the survey period. The error of calculation for the May data is less than 0.5°C.

Figure 10 also includes the calculations made for the Riverside Inlet Canal near Greeley, Colorado. The data are not suitable for publication as yet, because of some instrumental problems in the radiation and temperature measurements. The calculations were based on the adjusted data, which included a uniform 20 percent reduction of recorded incoming solar radiation values. The canal is 16 km long with little vegetation along both banks. The channel width ranged from 14 to 28 m, and the depth variation was between 0.6 and 1.2 m. The travel time, τ, for 16 km reach was about 5.5 hours. The temperature variation within a cross section was negligible except near the entrance to the canal. The large diurnal fluctuation in T_n is caused mostly by that of net incoming radiation. The calculation was based on $\Delta\tau=¼$ hours and $N=1.5\cdot10^{-8}$ kg·m^{-1}· newton^{-1}. The agreement between observed and calculated T_n is satisfactory.

In summary, the one-dimensional thermal equation, in conjunction with surface exchange equations, appears to provide a workable model for the natural temperature data available in this study. On the other hand, some questions on the transverse variation of temperature as well as the magnitude of mass transfer coefficients are not adequately answered by the present analysis.

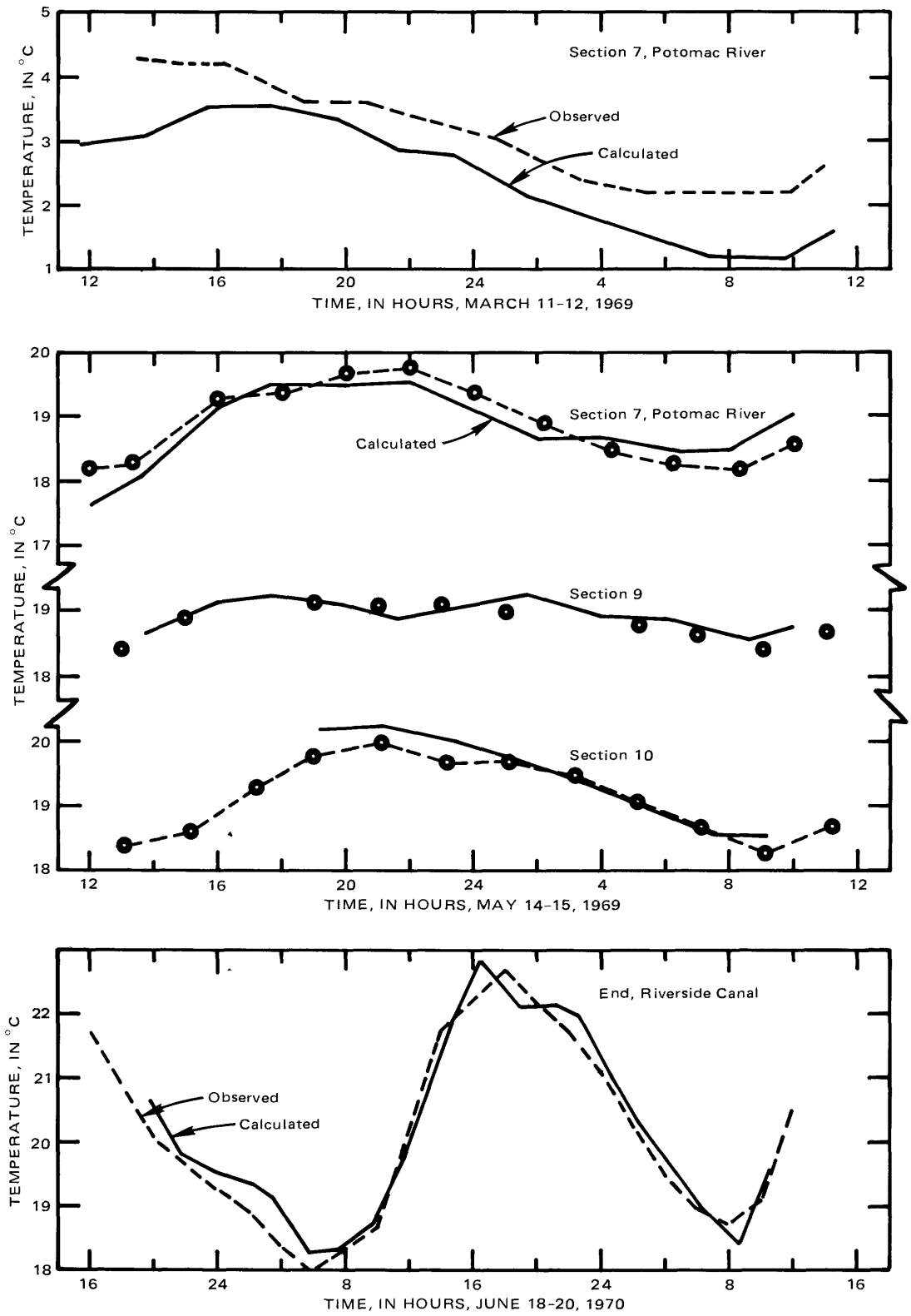

FIGURE 10.—Comparison of observed and calculated natural water temperatures, the Potomac River below Dickerson Power Plant, Maryland, 1969 and the Riverside Inlet Canal near Greeley, Colorado, 1970.

Note that the calculation based on the homogeneous stream model, equation 38, is much simpler than that based on the Lagrangian model, equation 39. All data required for equation 38 can be collected at one loca-

tion, whereas the data for equation 39 include travel time, τ, to various location and boundary temperature $T_{no}(0,t)$. Decisions as to which method to use in a particular problem depend on the availability of hydraulic information on the reach of concern. For most streams studied in this report, thermal homogeneity of natural temperature could be assumed without causing excessive errors. All streams had depth and other channel conditions comparable to those of the Potomac River.

ONE-DIMENSIONAL MODEL OF EXCESS TEMPERATURE

PRELIMINARY CONSIDERATIONS

In general, the decision on whether to employ a one-dimensional model or a two-dimensional model must be specific to each problem of interest. If a waste heat discharge constitutes the total stream discharge, there will of course be no need for a two-dimensional model. If a waste heat discharge is some fraction of the total stream discharge, however, the downstream thermal regime may be divided into near region, intermediate region, and far region (Jobson and Yotsukura, 1973). A one-dimensional model is most useful in the far region, where excess temperature is uniformly mixed in a cross section. Also, if the amount of waste heat remaining as the percentage of the initial load is the principal interest, as in the case of planning a series of power plants along a river, a one-dimensional approach will be adequate. A two-dimensional model, on the other hand, is useful in the intermediate region, where excess temperature is uniformly mixed over the depth but not in the transverse direction. The mixing zone or the plume configuration that can be defined by the model is of considerable importance in effluent management and control.

Of all the one-dimensional equations discussed thus far, two equations are petinent in the present context, namely, equation 5 as the basic starting equation and equation 24 as the simplified working model. Notice that T in equation 5 was defined as the cross-sectional average temperature without assuming the uniformity of temperature in the cross section. Therefore, equation 5 could be used in areas upstream of the far region. One must be aware in such uses that a cross-sectional average T must be used to calculate H. Because H is nonlinear with temperature, H based on average temperature may differ significantly from the width-averaged value of H. The observations of Yotsukura, Jackman, and Faust (1973) about errors due to nonlinearities showed that care should be exercised in using the one-dimensional model where lateral differences greater than 10°C exist.

Notice also that the longitudinal dispersion term was neglected in the derivation leading to equation 24. This is a valid assumption if a conservative solute is discharged into a steady uniform flow at a continuous uniform rate (Sayre, 1973). For nonconservative solutes such as excess heat, it is best to check this assumption for each specific problem by comparing two solutions, one with the dispersion term and the other without. For the present study, however, the use of equation 24 may be justified on the basis of Thomann's analysis (1973). According to this generalized analysis, the error from neglecting the dispersion term will increase as the magnitudes of three nondimensional parameters increase. Listed in the order of importance, these are: the dispersion parameter, KU_*/YV^2, the distance parameter, xU_*/YV, and the effluent parameter, $2\pi Y/U_* t_p$, where t_p is the period of cyclic change in effluent discharge rates. The present data indicate that the dispersion parameter is much less than 0.01 and the distance parameter is less than 1.0 considering the maximum reach length of about 30 km. These values, in reference to Thomann's numerical data, appear to be small enough to keep the error of equation 24 insignificant under most conditions. On the other hand, the effluent parameter for the present study is larger than Thomann's data. Its value is larger than 11.0, as any periods of waste discharge cycle will be less than 24 hours. When the period becomes on the order of 6 hours, the error will be significant.

The data obtained in this study indicate substantial differences in the distance required to attain uniform cross-sectional temperatures. Uniformity in the vertical direction is attained swiftly, and seldom are vertical temperature gradients measurable more than a few hundred metres downstream of the discharge point. Uniformity in the transverse direction requires much longer stream reaches, and the distance required varies greatly depending on the modes of thermal discharges and the alinement of channel. In the March and May surveys of the Potomac River, the heated plume had failed to reach the far bank of the river 35 km downstream from the discharge site. For all other streams, however, the excess temperature was uniformly mixed in a cross section a few kilometres downstream of the discharge site.

It is also worth noting that very long reaches are required to dissipate a large fraction of the heat added to a stream. This is particularly true in the case of waste heat discharges that increase the stream temperature only a few degrees centigrade. Figure 11 presents some typical plots of the percentage of excess heat remaining as a function of distance for the rivers where reaches 25 km and over were studied. In computing the heat remaining, it was necessary to assume that the natural temperature that would exist at a downstream point is the same as the observed temper-

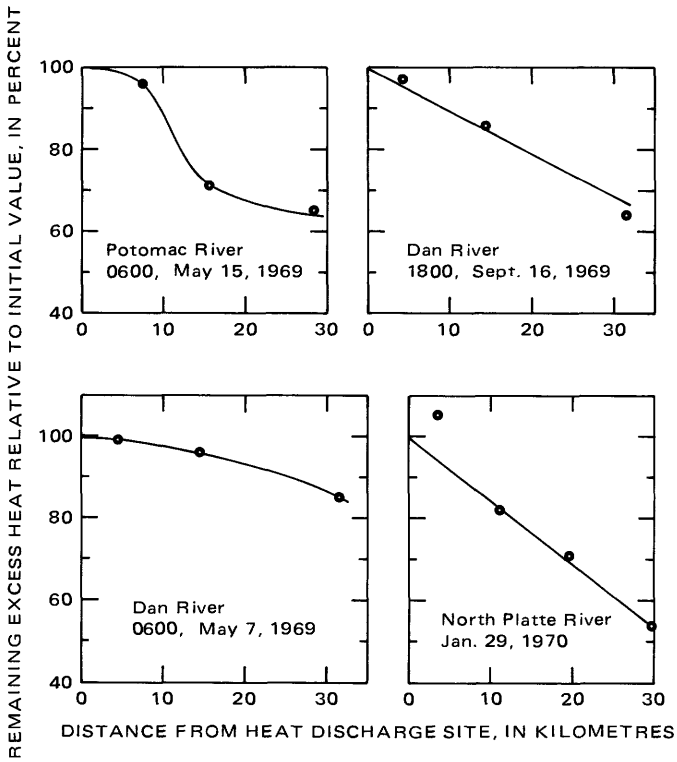

FIGURE 11.—Attenuation of remaining excess heat with distance downstream from heat discharge site.

ature above the discharge. As discussed above, this conjecture has been corroborated on the basis of observations from the Potomac River.

Perhaps the most significant feature of figure 11 is the great distance required to dissipate the added heat. All reaches were approximately 30 km in length, and yet no more than 50 percent of the heat had been dissipated in any case. These results are not entirely unexpected, as available models of heat exchange at the air-water interface are shown below to produce good temperature predictions, but they certainly belie the naive opinion that temperatures return to normal a few miles below a discharge.

All the graphs in figure 11 except that for the North Platte River represent observations made at a particular time at all cross sections, or Eulerian observations. Assuming steady meteorologic conditions, steady heat loading at the point of discharge, and uniform average velocity along the channel, one would expect the excess heat to decay as a constant negative exponential. Because there were considerable variations in the meteorologic conditions and probably in average stream velocity as well, one would expect some deviation from the decaying exponential, and this is evident in these figures. The figures point up the difficulties of applying any steady-state thermal models such as Eulerian exponential decay model of heat dissipation. If meteorologic conditions and average stream velocity are not constant, as is usually the case, it is most important to calculate excess temperature at the downstream point by solving transient thermal balance equation. This need is further amplified in field problems, in which waste discharge rate may vary a great deal with time, and meaningful pictures of heat dissipation can only be obtained by the above approach.

DESCRIPTION OF COMPUTATIONAL PROCEDURES

A Lagrangian form of solution to equation 24 has been given previously as equation 31. In a more commonly used form, it is

$$T_e(t) = T_{eo}(t_o) \exp\left(-\int_0^\tau \frac{U_*}{Y} d\tau'\right), \tag{31}$$

where t_o is the time when a particular packet of waste water with excess temperature T_{eo} leaves the effluent site, τ is the travel time measured relative to t_o, and $t=\tau+t_o$ as defined by equation 29. All the results discussed below were generated using some variation of this solution.

Before calculations can be undertaken, the input data must be put in a manageable form, because temperature data and meteorologic data collected at various times are quite cumbersome to use in the raw form. The temperatures and meteorologic variables were interpolated to each quarter hour and meteorologic conditions were assumed constant during each 15-minute interval. Estimated travel times were rounded off to the nearest quarter hour.

Starting with a packet having a given excess temperature at time t_o, equation 31 is employed to calculate the excess temperature of the same packet at $t_o+\Delta\tau$ where $\Delta\tau=15$ minutes. The calculated temperature at $t_o+\Delta\tau$ may then be used together with equation 31 and meteorologic data to calculate T_e $(t_o+2\Delta\tau)$. This procedure is repeated, starting with another water packet leaving the discharge site 15 minutes later than in the previous claculation. Repeating this procedure as many times as available data permit generates a calculated temperature history at the downstream section.

The Lagrangian solution method indicates that if the first excess temperature data at the discharge site is available at t_o, the first time at which downstream temperature may be calculated is at $t_o+\tau$ where τ is the travel time. Thus, observed downstream temperatures between t_o and $t_o+\tau$ may not be compared with calculated temperatures. As the Data Report describes, however, the decision to impose a uniform data collection period of 24 hours on all thermal surveys was made prior to the choice of predictive models. Accord-

ingly, application of the Lagrangian method is restricted to a reach with the travel time less than 24 hours. This inconvenience, however, was more than compensated by an advantage of the Lagrangian solution; that is, one is able to assess surface heat dissipation closely by following moving water masses with known initial excess heat.

Several approximations, which are required in order to complete the above calculation, should be discussed. First, in computing actual water temperatures at a downstream cross section, the natural temperature must be added to the excess temperature. Because no other data on natural temperature were available, the upstream temperature was taken to be the natural temperature that would exist at all downstream points in the absence of waste heat discharge. The limitations on this assumption have been discussed in the section on the "Analysis of Natural Temperature."

It is also necessary to estimate the travel time and average depth for each reach. The travel time may be estimated by dividing the length of the reach by the average velocity for the reach. Since complete stream discharge measurements were available at most cross sections, the average velocity at each cross section was calculated by dividing total discharge by total cross-sectional area of the reach. The average velocity for the reach may then be calculated as the average of the velocities at the upstream cross section and downstream cross section. This method can lead to rather serious errors if, as may well be the case, the channel geometries at the upstream and downstream cross sections are not typical of the reach as a whole. Average depth for the reach could also be calculated by taking the average of the average depths calculated from the discharge measurement at the upstream and downstream cross sections. This would again be of questionable accuracy.

In order to alleviate the above errors, use is made of the following relation among discharge, travel time, and reach volume,

$$Q\tau = A_s Y, \tag{40}$$

where A_s is the total surface area of the reach and the depth Y is defined such that $A_s Y$ represents the reach volume. Letting $\tau = n\Delta\tau$ and substituting these expressions into equation 31,

$$T_e(t_o+\tau) = T_{eo}(t_o)\ \exp\left(-\frac{A_s}{nQ}\sum_{i=1}^{n} U_{*_i}\right), \tag{41}$$

where U_{*_i} is a transient value of U_* for the i-th $\Delta\tau$ period. Note that Q and A_s can be determined accurately from field data and maps. Equation 41 was the form actually used in calculation.

One additional specific approximation should be mentioned. Equation 7 for natural temperature is transparent to the phase transition that actually occurs at 0°C. Negative values of H can result in temperatures less than 0°C were the water not to freeze. It is this hypothetical negative temperature, and not the freezing point of water, which must be used in cases where a stream is partially frozen and at 0°C. To do otherwise would require that $H(T_n,t)\equiv 0$, which is clearly incorrect. This problem arises in the data from the North Platte River where the unaffected stream was indeed frozen and at 0°C.

For the North Platte River, it was necessary to calculate the hypothetical natural temperature as a function of time. This was done by applying the homogeneous stream method of natural temperature prediction using equation 37. Field radiometer data were employed, and the value of N, the mass transfer coefficient, used was $2.68\cdot 10^{-8}$ kg·m^{-1}·newton^{-1}. The initial condition for the integration was chosen to produce a slightly negative average value of H for a 24-hour period since field observations indicated an increased rate of ice formation. The predicted natural temperatures appear in table 1.

RESULTS AND DISCUSSION

One-dimensional temperature prediction was undertaken for all streams presented in the Data Report except the Holston River, where no discharge data were available, and the Potomac River, where two-dimensional analysis appeared to be more appropriate. These calculations employed the one-parameter evaporation and conduction model as shown in equations 14 and 18. In most cases, the value of N was $2.68\cdot 10^{-8}$ kg · m^{-1} ·newton^{-1}, hereafter referred to as the standard value for the mass transfer coefficient. In cases where other values were used, an explanation will accompany the discussion of these results.

Figures 12 and 13 present sketches of river alinement, cross-sectional location, and other pertinent information for all streams analyzed in the following section.

WHITE RIVER NEAR CENTERTON, INDIANA, 1969

The temperatures calculated using the Lagrangian one-dimensional model for the various downstream sections at the White River near Centerton, Indiana, are compared with observed temperatures in figures 14–16. The reach length was only 12 km. Therefore, little heat loss occurred, and only the results from sections 4 and 7 are presented to avoid congestion. The standard value of the mass transfer coefficient was employed. Heat loading varied somewhat during all three studies, and excess temperatures just below the

TABLE 1.—*Temporal variation of hypothetical natural temperature under freezing conditions, the North Platte River near Glenrock, Wyoming, January 28–29, 1970*

t in hours	T in °C
1400	0.00
1500	0.04
1600	0.08
1700	0.04
1800	−0.01
1900	−0.09
2000	−0.21
2100	−0.30
2200	−0.38
2300	−0.50
2400	−0.62
0100	−0.74
0200	−0.86
0300	−0.98
0400	−1.10
0500	−1.26
0600	−1.42
0700	−1.10
0800	−1.80
0900	−1.67
1000	−1.49
1100	−1.10
1200	−0.64
1300	−0.30
1400	−0.11

discharge site were 1.7–2.5, 5.5–6.4, and 3.0–4.4°C for the February, June, and October studies, respectively.

Figure 14 for the February study shows very good agreement between predicted and observed temperature at cross section 4 and good agreement at cross section 7 except during the immediate predawn period. Because this was a period of very light winds, it is unlikely that errors in the estimation of evaporation and conduction could have caused the deviation. It appears most likely that the deviation was caused by a failure in the assumption of constant natural temperatures along the reach.

Figure 15 shows the comparison of prediction with observation for the June study. The rate of cooling has been rather substantially underestimated during most of the study. The period of underestimation coincides very closely with the period during which observed winds dropped to less than 1 m·sec^{-1}. The observed wind velocities possibly were not characteristic of the winds that prevailed over most of the channel. The unexpectedly high dissipation rates could not be due to natural convection in this case, because water temperatures were nearly equal to air temperatures during some of this period.

Figure 16 shows the modeling results for the October study. Winds were high during the first 8 hours of the study although still less than 3 m·sec^{-1}. Excess temperatures were generally in the vicinity of 4°C at all cross sections. The amount of cooling appears to have been overpredicted rather than underpredicted during

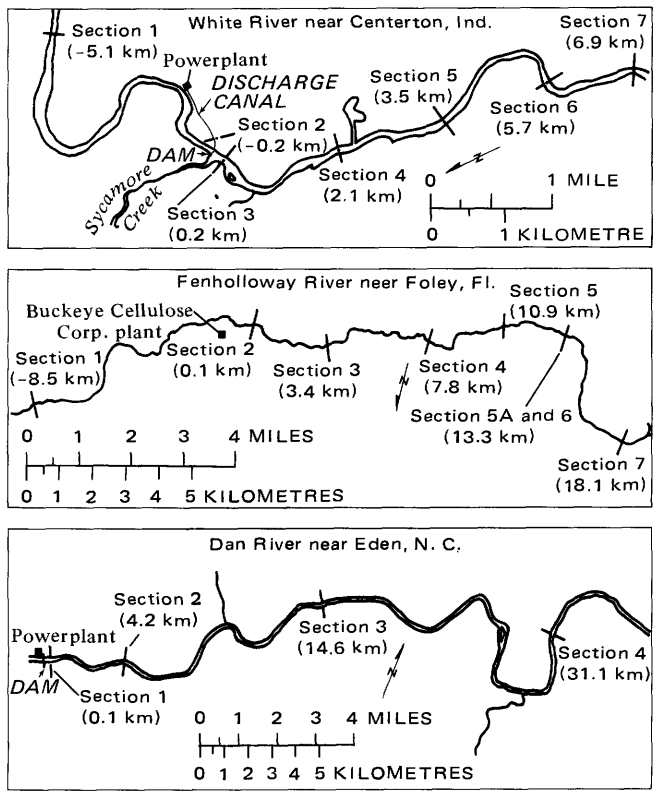

FIGURE 12.—Sketch of study reaches, I.

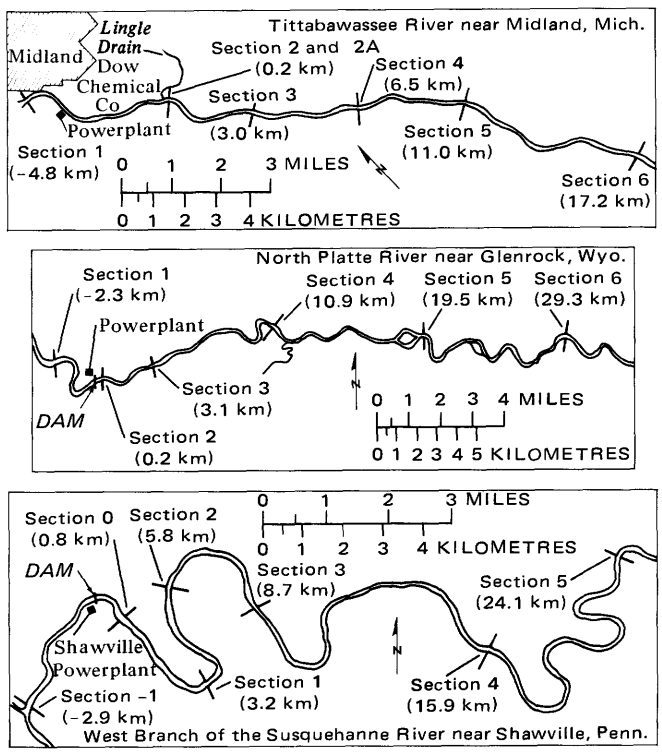

FIGURE 13.—Sketch of study reaches, II.

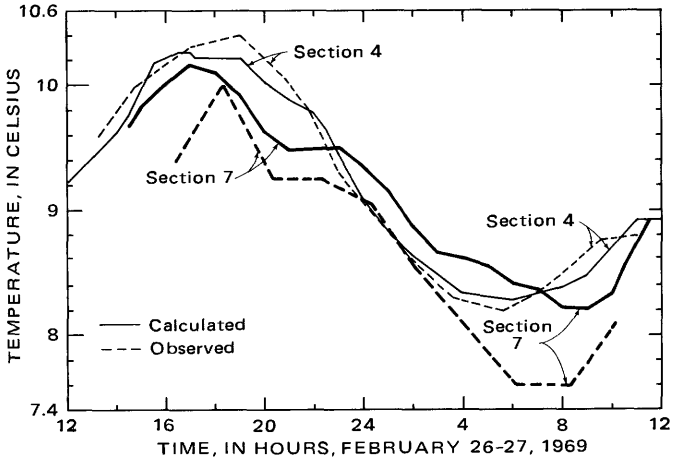

FIGURE 14.—Comparison of observed and calculated water temperatures, the White River near Centerton, Indiana, 1969.

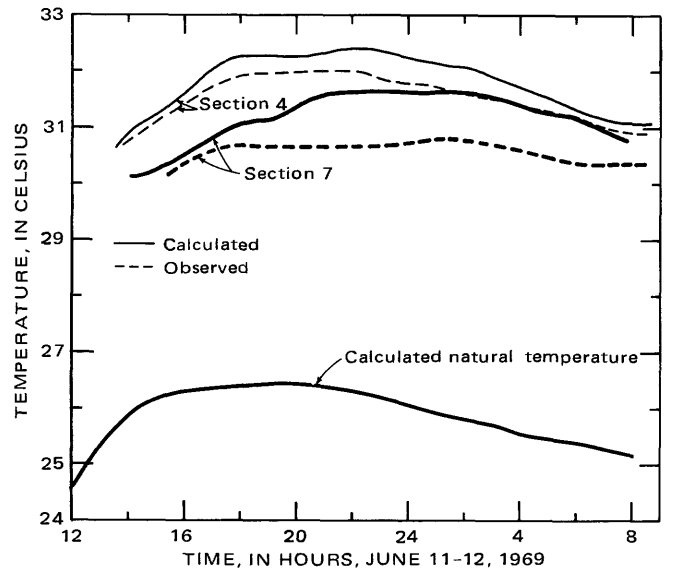

FIGURE 15.—Comparison of observed and calculated water temperatures, the White River near Centerton, Indiana, 1969.

the morning hours, when wind speeds were again very low. The cause is a decrease in measured natural temperature of 0.5°C between 0500 and 0700 hours. During the same period one would expect a similar decrease in the actual temperature at affected downstream sections, as no unusual transient had been observed moving downstream. This expected decrease in observed temperature is absent.

These data probably hold greater significance from the standpoint of fluctuations in natural temperature than they do from the standpoint of accuracy of the one-dimensional model, because of the short reach and travel time studies at the White River and the small dissipation. It is interesting to compare the fluctuations at the downstream sections with the fluctuations

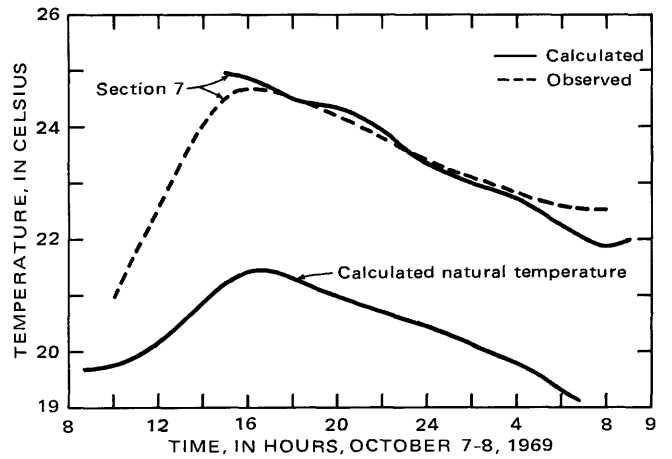

FIGURE 16.—Comparison of observed and calculated water temperatures, the White River near Centerton, Indiana, 1969.

at the upstream natural temperature cross section. Figure 17 plots the deviation of the natural temperature from its value of 2400 hours and the same deviations at the cross sections 3 and 7. Large deviations from the natural temperature pattern occur at cross section 3 in the morning hours of both days. Large deviations also occur at section 7 on the morning of the second day. These deviations are as great as 1.2°C. The assumption of the thermal homogeneity in natural temperature may have been the source of the errors in temperature prediction.

FENHOLLOWAY RIVER NEAR FOLEY, FLORIDA, 1969

The Fenholloway River near Foley, Florida, is interesting for several reasons. It is the smallest of the streams studied, unusually small for a stream receiving a waste heat discharge. Because of its small discharge and large heat loading, it had the largest excess temperatures of any stream studied, as high as 17°C. Finally, it had significant flow accretion in the reach studied. Most of the accretion was unmeasured, but there was one measured inflow from Waldo Spring which entered the river just downstream of section 5A. The temperature of the spring was about 21°C for both the March and June studies (it was not observed during the November study). The fact that the temperature was fairly constant, at about the mean annual temperature for the region, suggests that the spring was ground water outflow and, therefore, is representative of the temperature of any accretion resulting from ground-water pickup by the channel.

Figures 18–20 show comparisons of calculated and observed temperatures at the Fenholloway River. The starting point for the calculations was section 2, just downstream of the discharge. The reach studied was 18.1 km long. The standard value of the mass transfer coefficient was employed, although results indicate a

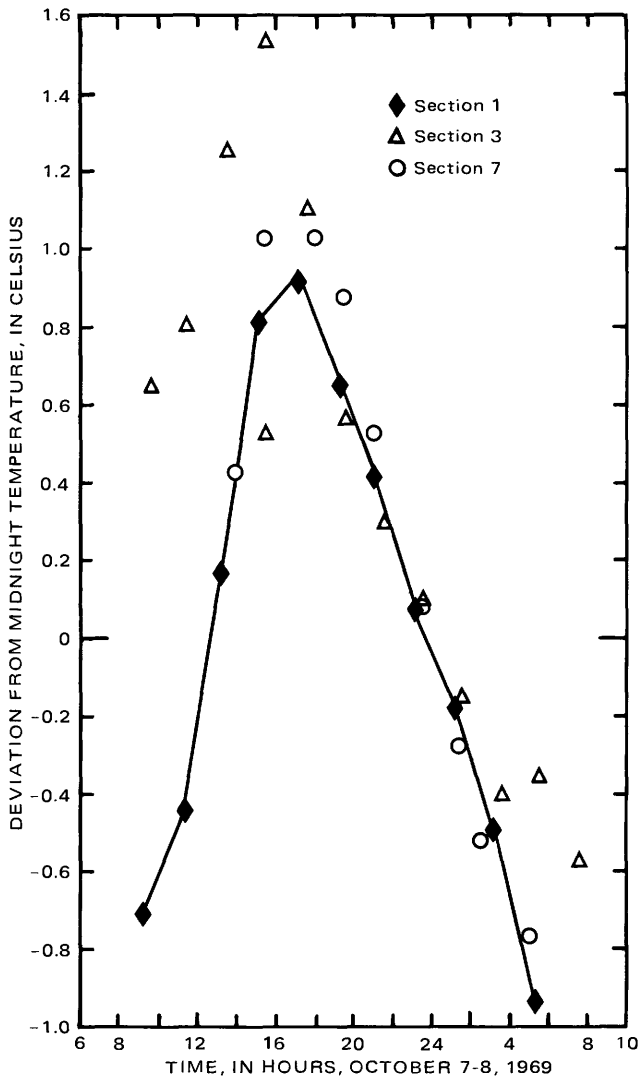

FIGURE 17.—Temporal variation of natural and heated water temperatures, the White River near Centerton, Indiana, 1969.

somewhat higher value might be justified. The water at the upstream end of the reach was generally warmer than the air.

All the studies reveal a dramatic overprediction of temperature. Errors as great as 4°C are found at the downstream sections. Much of the error appears to be due to the ground-water accretion. If it were assumed that all the accretion at section 7 occurred just before the section, mixing the cool ground water (computed as the difference between the discharge at section 7 and that at section 2), a cooling of 2°C for the March study and 5°C for the June study would be predicted. For the November study, section 5A replaced section 7 and a cooling of 2°C at this section would be predicted. These predictions compare fairly well with observed errors. Figures 21–23 present modified prediction which assumes a complete mixing of ground water and heated water. The agreement between calculated and observed temperatures is considerably better. The problems with the shapes of the time-temperature relationships for the March and November studies remain since they are not affected appreciably by the ground-water accretion correction. A tendency to underestimate cooling is still evident.

The cooling effect of the accretion is somewhat overpredicted if the accretion actually enters more or less uniformly along the channel, as is probably the case on the Fenholloway. In this case, the reduced excess temperature resulting from accretion to a heated packet near the source will cause a reduction in the heat losses from that packet. Therefore, the packet arriving at the end of the reach which has suffered the same apparent heat loss due to accretion as if the accretion all occurred at the most downstream point has suffered smaller losses to the atmosphere. This indicates a very significant under-estimation of heat transport at the air-water interface has occurred. This must, in large part, be due to the extremely unstable atmospheric conditions that prevailed.

The results of the November study in figure 20 reveal a peculiar and sharp increase in predicted temperature during the period from 1700 to 2400 hours at cross section 3. The calculated pattern then propagated to the downstream sections causing similar peaks later at successive sections. This was caused by a sharp decrease in wind velocity at about 1600 hours, which caused the calculated decrease in excess temperature between sections 2 and 3 to decrease from 1.5°C at 1700 hours to 0.5°C at 2400 hours. During the same period the excess temperature at section 2 also increased nearly 1°C.

The great sensitivity to changes of wind speed is the result of predicting evaporative and conductive heat losses using the one parameter mass transfer formula, equations 22 and 23. The observed temperature shows only a slight increase caused by the increased heat loading. It appears that cooling did not decrease dramatically during this period. This is probably the result of large evaporation and conduction losses caused by free convection. During this period the water was about 15°C warmer than the air.

DAN RIVER NEAR EDEN, NORTH CAROLINA, 1969

The comparisons of predicted and observed temperatures for the three studies of the Dan River near Eden, North Carolina, are shown in figures 24–26. The starting point for calculations was section 1 just downstream of the discharge. The reach was the longest studied, 31 km. Heat loading was fairly constant during all studies. Excess temperatures were about 2.8, 4.2, and 6.5°C for the April, May and October studies,

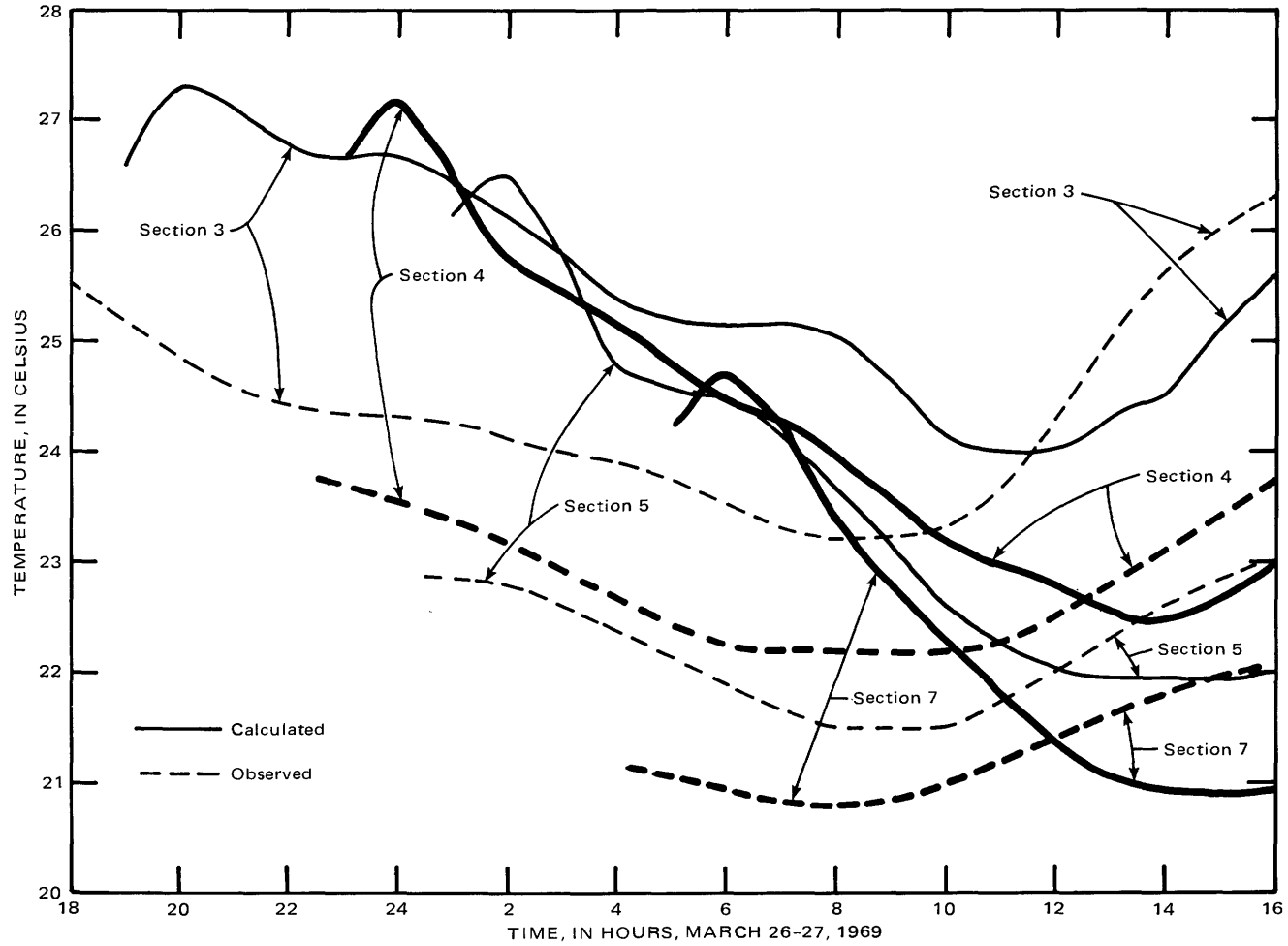

FIGURE 18.—Comparison of observed and calculated water temperatures, the Fenholloway River near Foley, Florida, 1969.

respectively. The standard value for the mass transfer coefficient was used in all cases. The river flow is regulated, and only small changes in flow were observed during the studies. These changes should have little effect on the one-dimensional modeling, changing only the travel time. As the estimates of travel time used here are somewhat crude, it is doubtful that the slight discharge changes would affect this estimate.

The predictions for the April study shown in figure 24 are in excellent agreement with measured values. The rapid rise in temperature at section 2 in the afternoon of the first day is correctly convected downstream producing an increase in temperature at section 4 during the early morning hours. This rather unusual increase was borne out by measurements.

As in the case of the Fenholloway River, there were rapid changes in wind speed during the April study. The wind decreased from nearly 6 $m \cdot sec^{-1}$ to 1 $m \cdot sec^{-1}$ between 1500 and 1900 hours and then rose less dramatically from 0600 to 1000 hours of the second day. However, unlike the Fenholloway River, excess temperatures were only about 3°C. Thus, excess temperature would decrease less than a degree Celsius in any reach, and changes due to wind would be only a fraction of a degree. In addition, since air temperatures exceeded water temperatures, evaporation and conduction should not be enhanced by free convection.

The predictions for the May study are also good. There is a sharp decrease in temperature at section 2 at about 2100 hours that does not agree with observation. This was the result of a 0.75°C drop in observed temperature at section 1, from which excess temperature is calculated. The results seem to indicate that this drop may have been due to observational error. There is some underestimation of cooling at sections 3 and 4. Air temperatures were lower than water temperatures from 1800 hours until the conclusion of the test, and some free convection enhancement of evaporation and conduction rates may have occurred.

TITTABAWASSEE RIVER NEAR MIDLAND, MICHIGAN, 1969

The comparisons of predicted and observed tempera-

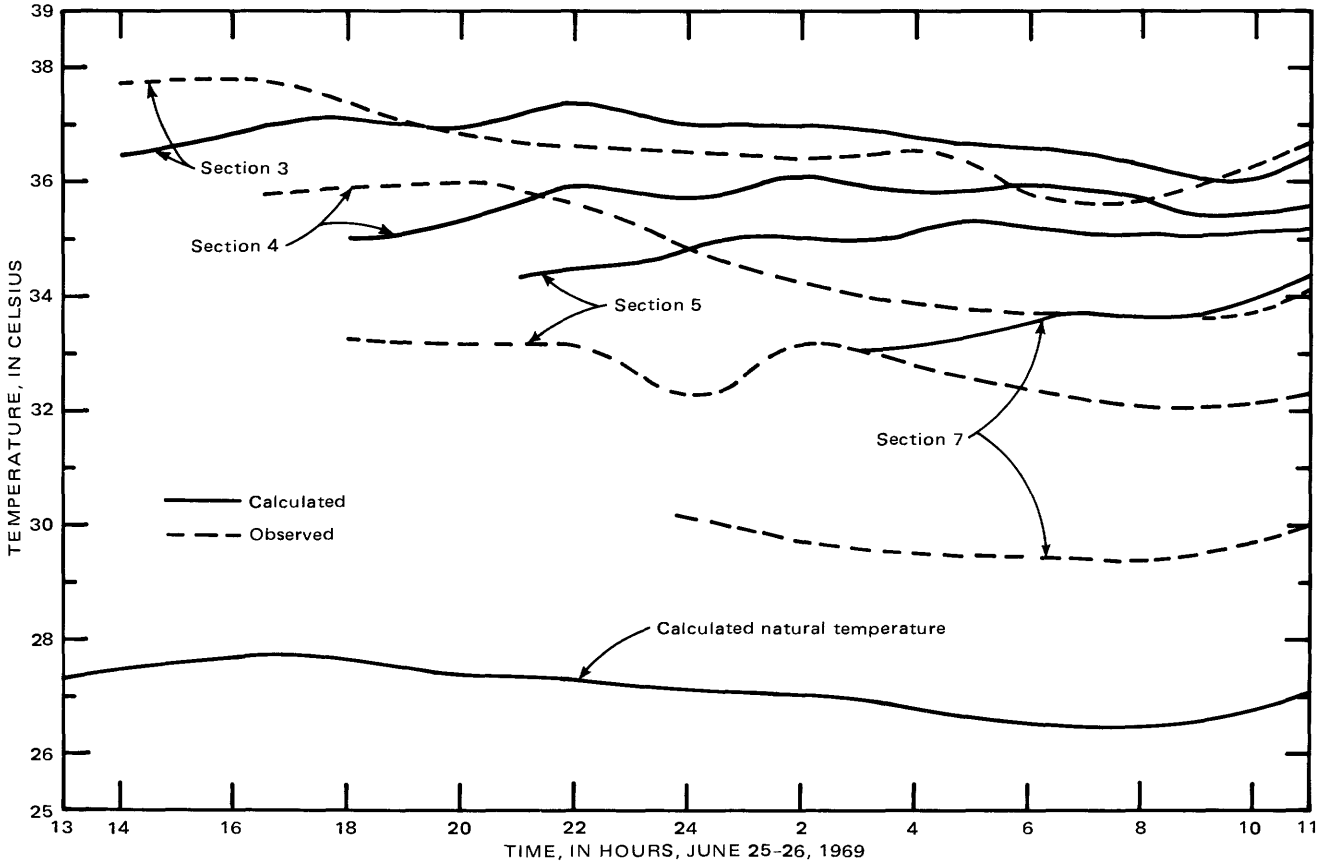

FIGURE 19.—Comparison of observed and calculated water temperatures, the Fenholloway River near Foley, Florida, 1969.

tures for the two studies of the Tittabawassee River near Midland, Michigan, are shown in figures 27 and 28. Calculations started at section 2 just downstream of the discharge site. The study reach was 11.0 km long in September and 17.2 km in October. The standard value of the mass transfer coefficient was used. Heat load varied somewhat and excess temperatures ranged from 6 to 8°C for the September study and 2.5–4°C for the October study. Air temperatures were substantially less than water temperatures for both studies.

The predictions for the September study are generally good. Because the one-dimensional model employed here does not account for longitudinal dispersion, the sharp peak in initial temperature, which appeared at the section just below the discharge point at 1030 hours, was propagated downstream by the computer solution with no appreciable spreading. The measured values clearly show that the dispersion actually occurred. There is also a slight tendency to overestimate cooling in spite of the fact that air temperatures were 5–10°C less than water temperatures.

The predictions for the October study are less satisfactory. The excess temperatures were much smaller but increased by about 60 percent during the study period. The downstream convection of this change appears to have caused some of the error. However, there was indication of a large thermometry error. The observed temperatures at section 2 were about 0.5°C less than those observed at section 3 during the early morning hours when the heat load was relatively constant. If the temperature observed at section 3 is assumed to represent the correct temperature at section 2, this would increase the initial excess temperatures by 0.5°C and effectively raise the calculated results at sections 3, 5, and 6 by that amount. Clearly a correction of this magnitude would cause a considerable improvement in the agreement of calculated and observed temperatures.

NORTH PLATTE RIVER NEAR GLENROCK, WYOMING, 1970

The comparison of predicted and observed temperatures for the North Platte River near Glenrock, Wyoming, is shown in figure 29. This study was performed in January and is the only data collected during the winter. Calculations were started at section 2 just below the discharge site. The reach was 29.8 km long. The standard value of the mass transfer coefficient was employed. Significant variations in heat loading were

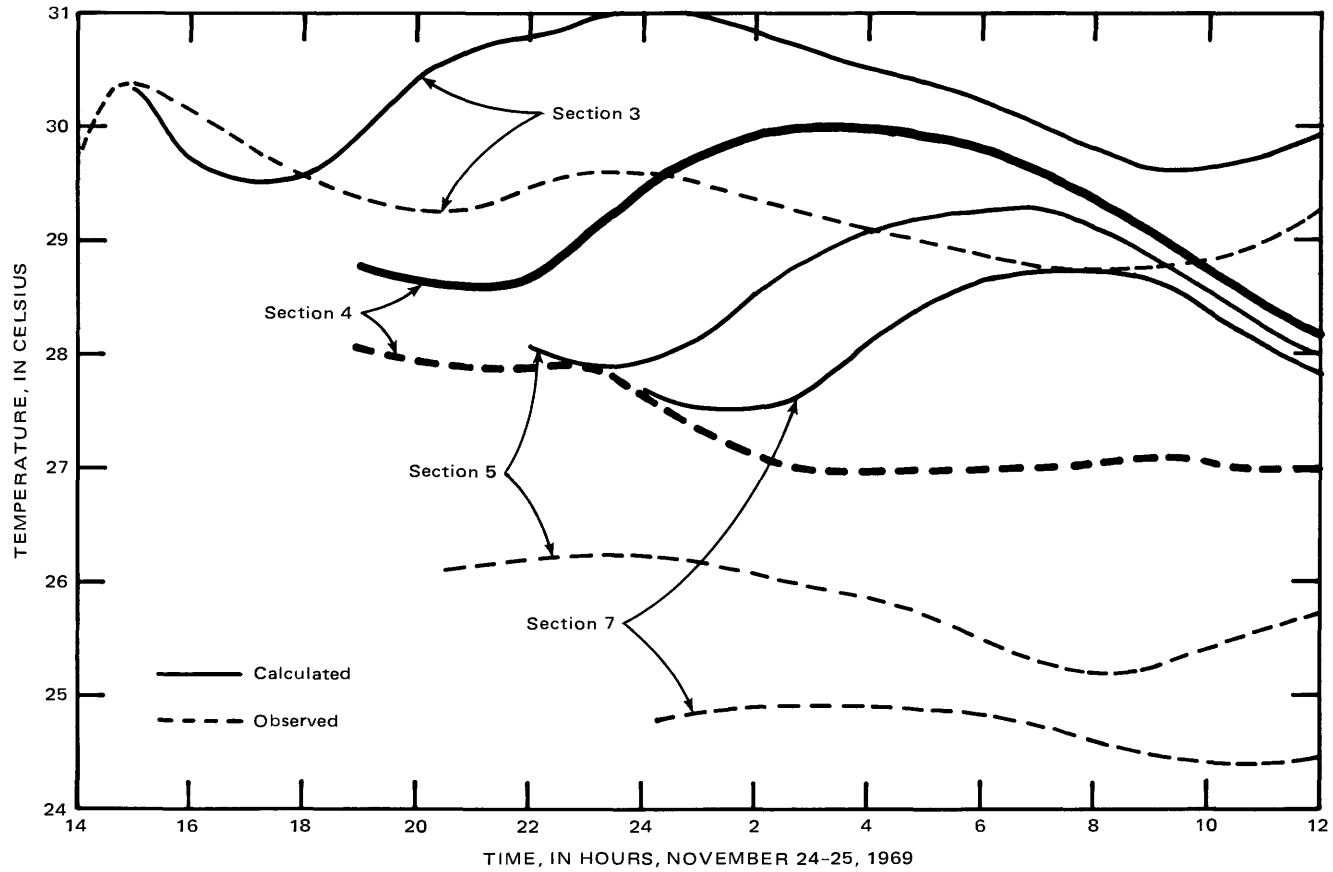

FIGURE 20.—Comparison of observed and calculated water temperatures, the Fenholloway River near Foley, Florida, 1969.

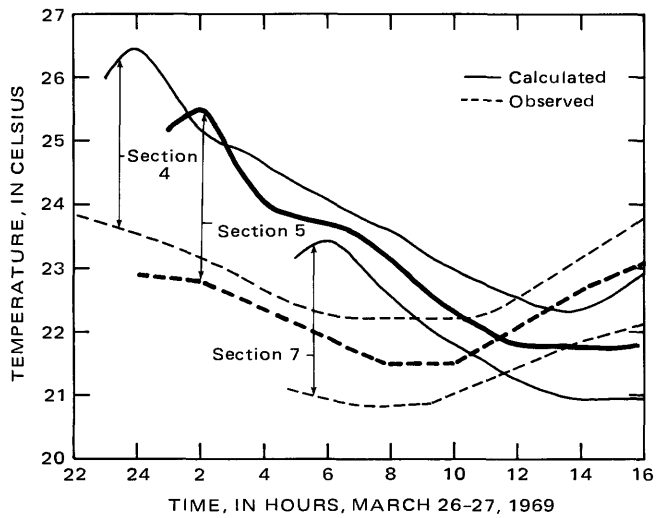

FIGURE 21.—Comparison of observed and calculated water temperatures, the Fenholloway River near Foley, Florida, 1969. Calculations are modified to account for ground-water accretion.

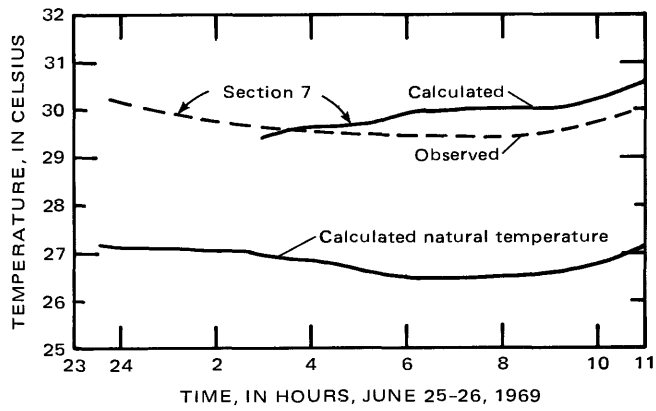

FIGURE 22.—Comparison of observed and calculated water temperatures, the Fenholloway River near Foley, Florida, 1969. Calculations are modified to account for ground-water accretion.

encountered during this study with excess temperatures varying from 7.4 to 9.0°C. The air temperature remained well below freezing throughout the study, ranging from -3.3 to -10.8°C. The river was frozen above the discharge with the flowing water temperature at 0°C. This required the prediction of the hypothetical negative natural temperature as discussed earlier.

The prediction is generally quite good. There is a sharp drop at section 3, starting at about 0100 hours,

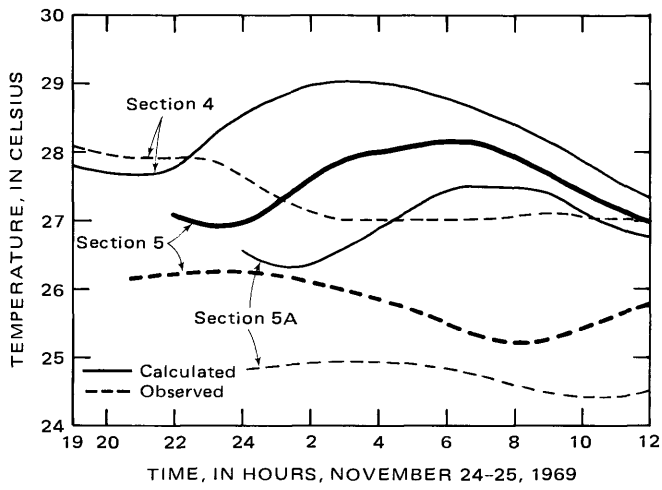

FIGURE 23.—Comparison of observed and calculated water temperatures, the Fenholloway River near Foley, Florida, 1969. Calculations are modified to account for ground-water accretion.

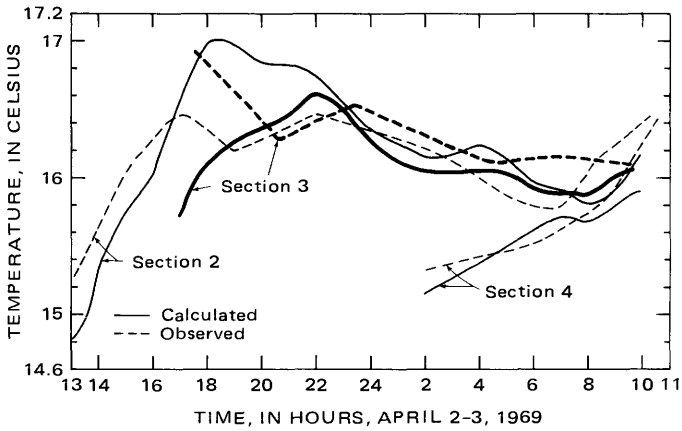

FIGURE 24.—Comparison of observed and calculated water temperatures, the Dan River near Eden, North Carolina, 1969.

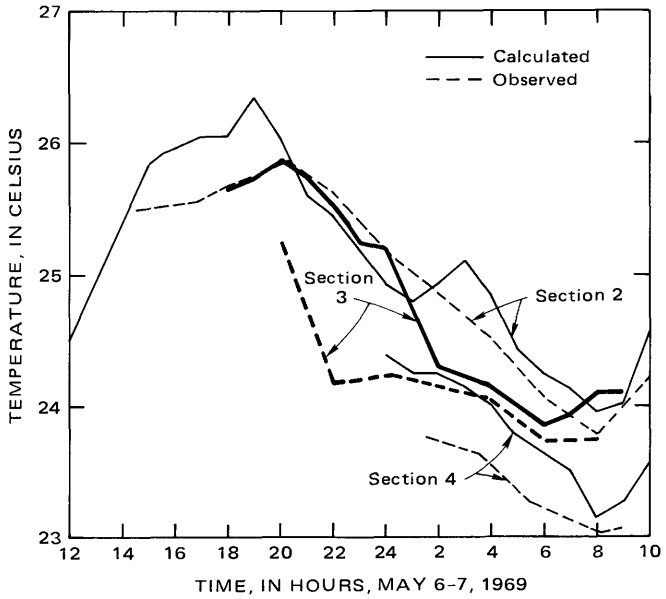

FIGURE 25.—Comparison of observed and calculated water temperatures, the Dan River near Eden, North Carolina, 1969.

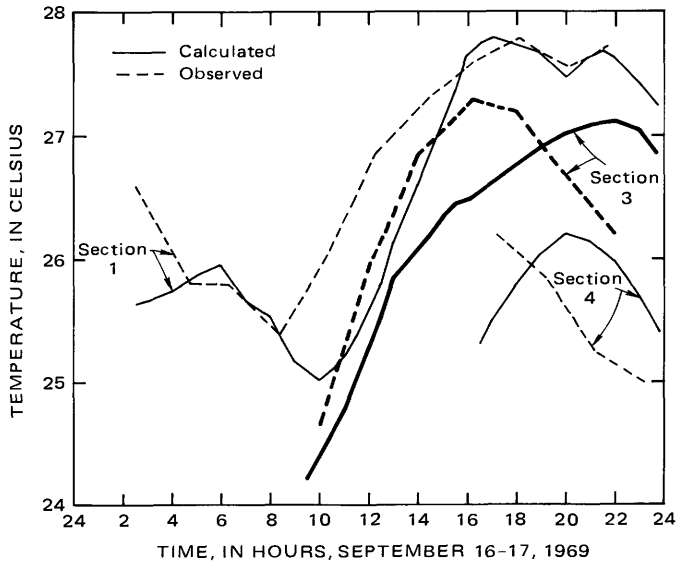

FIGURE 26.—Comparison of observed and calculated water temperatures, the Dan River near Eden, North Carolina, 1969.

which does not appear in the data. This was induced in the solution by a drop of 0.8°C in the excess temperature at the starting point, section 2, occuring between 2400 and 0200 hours. It is possible that the temperature measurement at 0200 hours, which was considerably lower than that at 2400 hours and that at 0355 hours, may have resulted from temporary input conditions and was not representative of the temperature at section 2 from 0100 to 0300 hours. The prediction would surely have been better had the temperature at 0200 hours at section 2 been 0.5°C higher. There was also an increase in wind speed from 2 $m \cdot sec^{-1}$ to 4 $m \cdot sec^{-1}$ that occurred at about 0100 hours and caused a sharp reduction in the value of T_e at section 3.

There is some overestimation of cooling, particularly during the early morning hours. During this period, ice formation occurred at the right bank (discharge was concentrated on the left bank). This condition ceased somewhere between sections 3 and 4 where mixing supplied enough heat at the right bank to prevent ice formation. There is no quantitative information on the amount of ice that formed. However, any ice formation has the effect of liberating heat to the remainder of the system and would cause observed temperatures to be higher than expected. The melting of ice, which was complete by 1100 hours, would require energy from the rest of the system. This would lower the temperature or, more precisely, slow the rate of increase of tempera-

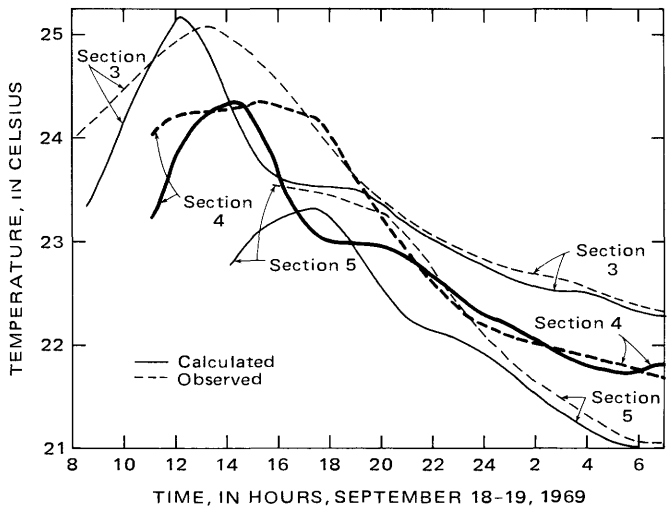

FIGURE 27.—Comparison of observed and calculated water temperatures, the Tittabawassee River near Midland, Michigan, 1969.

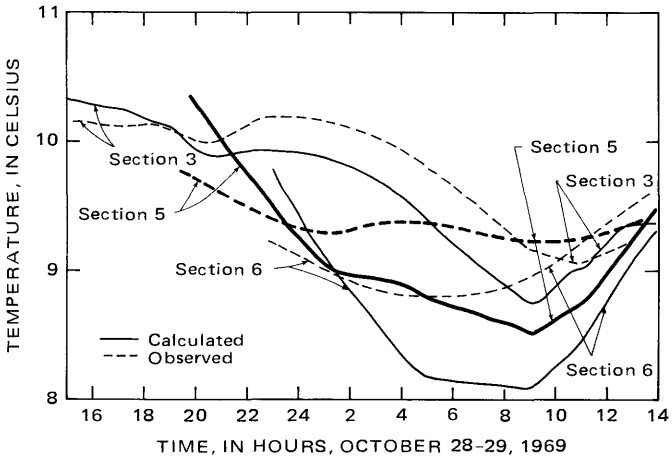

FIGURE 28.—Comparison of observed and calculated water temperatures, the Tittabawasee River near Midland, Michigan, 1969.

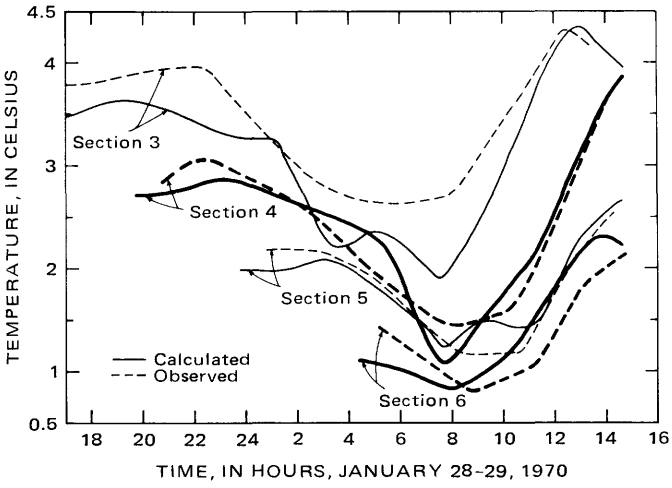

FIGURE 29.—Comparison of observed and calculated water temperatures, the North Platte River near Glenrock, Wyoming, 1970.

ture in the postdawn hours, and thereafter prediction and observation should agree. Excepting this ice formation, the estimate of cooling appears to have been quite good.

WEST BRANCH OF THE SUSQUEHANNA RIVER NEAR SHAWVILLE, PENNSYLVANIA, 1962

The comparison of predicted and observed temperatures for the West Branch of the Susquehanna River near Shawville, Pennsylvania, is shown in figure 30. Calculations were started at section 0 just below the discharge site. The total reach length was 24.1 km. The standard value for the mass transfer coefficient was used. Excess temperatures were quite high, ranging from 12 to 13.5°C at section 0. Air temperatures were less than water temperatures at all times.

The prediction is generally quite good and, in particular, the average dissipation seems to have been estimated quite well. Nevertheless, because of the high excess temperature, a problem similar to that encountered during the November study on the Fenholloway River can be noted. A sharp decrease in wind speed at about 1800 hours resulted in such a great rate of increase in the excess temperature that the predicted total temperature started rising in spite of decreasing natural temperature. After the low windspeed had persisted for a period equal to a travel time, all the heated water packets arriving at section 1 had experienced only low windspeeds and excess temperature stabilized, and the total temperature decreased owing to decreasing natural temperature.

Unlike the November study on the Fenholloway River, there is no appearance that evaporation and conduction have been underestimated using standard mass transfer expressions. In light of the highly unstable conditions that existed, this is difficult to understand.

CONCLUSIONS REGARDING ONE-DIMENSIONAL MODELING

For most of the sites studied, the one-dimensional, nondispersive Lagrangian model would appear to be adequate for downstream temperature prediction. Rapid changes in heat loading rates may induce longitudinal temperature gradients so sharp that dispersion must be considered. This is evident in the results for the September study on the Tittabawassee River.

In most cases the conventional mass transfer formulation of equation 14 appears adequate using a mass transfer coefficient of $2.68 \cdot 10^{-8}$ kg·m^{-1}· newton^{-1}. In the case of the Fenholloway River, this value is apparently too small. This is not entirely surprising in light of the area dependence of the mass transfer coefficient as given by equation 15 and the fact that the Fenhol-

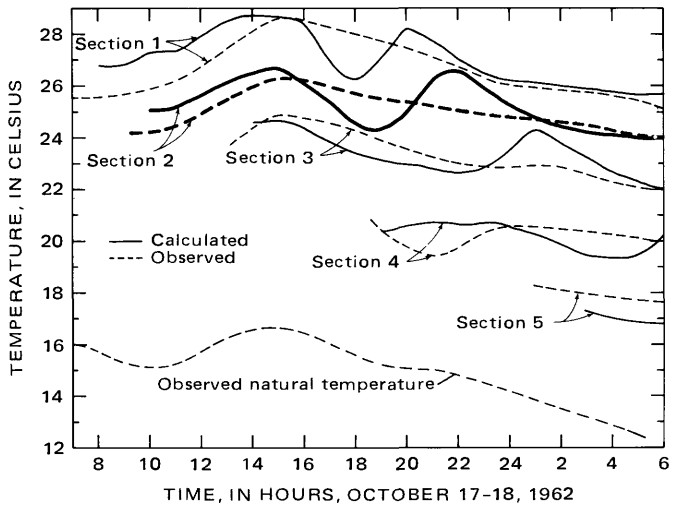

FIGURE 30.—Comparison of observed and calculated water temperatures, west branch of the Susquehanna River near Shawville, Pennsylvania, 1962.

loway River was by far the smallest stream studied. It would also appear that the predicted mass transfer is too sensitive to changes in wind velocity where unstable atmospheric conditions prevail. This is particularly evident in the results from the Fenholloway River and the West Branch of the Susquehanna River, where very large excess temperatures made the sensitivity of heat exchange to changes in wind velocity obvious.

The calculations strongly support the conclusion, evident from a consideration of the data, that very long reaches are required to dissipate the majority of the waste heat added to a stream. This is particularly true if the excess temperature at the point of discharge is low—a requirement now imposed by most states on waste heat discharges. Only in the cases of the Fenholloway River and the West Branch of the Susquehanna River were heat losses at the end of the study reach greater than 50 percent of the heat added. In both cases the excess temperatures were far above those now permitted by most states.

The above conclusion suggests that calculations such as proposed here may be necessary in the operation and siting of power plants downstream of existing waste heat sources. If regulations are designed to permit excess temperature no greater than some specified figure, a downstream facility should not be permitted that full figure if an upstream discharge exists. But since neither the natural nor the excess temperature can be measured immediately above the downstream facility, either the natural temperature or the excess temperature at that point will require calculation. If the stream thermal regime is reasonably homogeneous, the excess temperature is the clear choice.

TWO-DIMENSIONAL MODEL OF EXCESS TEMPERATURE

MODEL FOR A STEADY UNIFORM CHANNEL

The two-dimensional equation for thermal balance in a natural water body was derived previously as equation 4. In order to develop a working model for natural streams, it must be simplified as for the one-dimensional models. The source-sink term, S, and the bottom heat exchange term, H_{bot}, are neglected. The flow is assumed to be steady uniform so that the depth-averaged transverse velocity, v_z, is nonexistent and Y and v_x are sole functions of z. The longitudinal dispersion term will be neglected on the grounds discussed previously. All these assumptions reduce equation 4 to

$$\frac{\partial T}{\partial t}+v_x\frac{\partial T}{\partial x}=\frac{1}{Y}\frac{\partial}{\partial z}\left(YK_z\frac{\partial T}{\partial z}\right)+\frac{H}{\rho C_p Y}. \qquad (42)$$

In equation 42, T is the depth-averaged water temperature, v_x the depth-averaged longitudinal velocity, and K_z is the depth-averaged thermal dispersion coefficient. The symbol H is the surface heat influx and Y is the depth.

Following the same approach as in the one-dimensional model, the excess temperature T_e is defined as $(T-T_n)$, where T_n is the temperature that would occur under the same meteorologic and hydraulic conditions if there was no waste heat discharge. The surface influx will be linearized by means of equations 24, 25, and 26. The resulting equation for T_e is

$$\frac{\partial T_e}{\partial t}+v_x\frac{\partial T_e}{\partial x}=\frac{1}{Y}\frac{\partial}{\partial z}\left(YK_z\frac{\partial T_e}{\partial z}\right)-\frac{U_* T_e}{Y}. \qquad (43)$$

Equation 43 forms a boundary value problem in a steady uniform flow when combined with proper boundary conditions. Because of the dependence of v_x, Y, and K_z on z, however, a closed form solution is not obtainable for equation 43, and it must be solved numerically.

A simpler approach to equation 43 is possible if the boundary condition is simplified such that waste water discharge and excess temperature are assumed to be steady at the discharge site. It consists of combining the one-dimensional exponential decay model for surface heat dissipation with the two-dimensional steady-state diffusion model developed by Yotsukura and Cobb (1972). Notice that if the excess heat were conservative so that $U_*=0$, equation 43 is reduced to a steady-state equation

$$v_x\frac{\partial T'_e}{\partial x}=\frac{1}{Y}\frac{\partial}{\partial z}\left(YK_z\frac{\partial T'_e}{\partial z}\right). \qquad (44)$$

Suppose that T'_e, the hypothetical excess temperature without decay, satisfies equation 44. Because the heat decay due to surface dissipation is a slow process relative to the heat transport by convection and diffusion, its parameter U_*/Y may be approximated by $U_*/\{Y\}$, which is a function of time alone if $\{Y\}$, the cross-sectional average depth, is constant. Accordingly a solution to equation 43 is proposed as

$$T_e(x,z,t)=T'_e(x,z)\exp\left(-\int_{t_o}^{t}\frac{U_*}{\{Y\}}dt'\right). \tag{45}$$

Equation 45 can be shown to satisfy equation 43 if the heat decay term is replaced by $U_*T_e/\{Y\}$ in equation 43.

Even though equation 45 is derived conceptually from the form of product solutions frequently used in the diffusion of reacting solutes (Crank, 1967), it could also be viewed as a combination of an Eulerian solution to diffusion and a Lagrangian solution to dissipation. It is similar to the approach used by Yeh, Verma, and Lai (1973) in the prediction of excess temperature for a cooling pond. Equation 45 should be considered as an approximation to what is physically going on rather than as a rigorous solution to a boundary value problem. The decay term in equation 45 will be calculated in terms of travel time in the same Lagrangian sense as in the one-dimensional model.

As for steady-state solutions to equation 44, the approach used by Yotsukura and Cobb (1972) consists of transforming equation 44 into

$$\frac{\partial T'_e}{\partial x}=\frac{\partial}{\partial q}\left(K_z v_x Y^2\frac{\partial T'_e}{\partial q}\right), \tag{46}$$

where q is the partial cumulative discharge measured from one side of a cross section and is defined by

$$q=\int_o^z v_x Y\,dz'. \tag{47}$$

Note that $q=Q$ when the integration in equation 47 is carried over the entire cross section. Equation 46, in which q replaces z as the independent variable, is simpler to handle than equation 44, because the convective velocity is reduced to unity. The new coefficient in the dispersive term of equation 46, $K_z v_x Y^2$, may be approximated by a constant cross-sectional average value, $\{K_z v_x Y^2\}$, so that the following approximate solution is given to equation 46:

$$T'_e(\alpha,q')=\frac{1}{2}T_{eo}\left[\sum_{n=0}^{\infty}\sum_{j=1}^{2}\left\{\operatorname{erf}\frac{\alpha(q'_{s2}+2n+\delta_j q')}{\sqrt{2}}-\operatorname{erf}\frac{\alpha(q'_{s1}+2n+\delta_j q')}{\sqrt{2}}\right\}\right.$$

$$\left.+\sum_{n=1}^{\infty}\sum_{j=1}^{2}\left\{\operatorname{erf}\frac{\alpha(q'_{s2}-2n+\delta_j q')}{\sqrt{2}}-\operatorname{erf}\frac{\alpha(q'_{s1}-2n+\delta_j q')}{\sqrt{2}}\right\}\right]. \tag{48}$$

The symbol T_{eo} is the steady excess temperature at the initial cross section, where Q_s is the steady excess water discharge rate and $\rho C_p Q_s T_{eo}$ represents an inflow rate of excess heat. Summation with respect to index j is defined by $\delta_1=+1$ and $\delta_2=-1$. The symbol α is a nondimensional longitudinal distance parameter,

$$\alpha=\sqrt{Q^2/2x\{K_z v_x Y^2\}}, \tag{49}$$

while q', fractional cumulative discharge q/Q, represents a transverse position. The symbols q'_{s1} and q'_{s2} are fractions q_{s1}/Q and q_{s2}/Q respectively, where q_{s1} and q_{s2} represent the two ends of a part of streamflow contaminated by excess temperature at the initial section and $q_{s2}-q_{s1}=Q_s$.

By means of field tracer tests Yotsukura and Cobb (1972) showed that equation 48 is quite satisfactory for a number of straight uniform channels and is also usable in a moderately meandering reach of the Missouri River.

MODEL FOR A STEADY NATURAL STREAM

In applying equation 45 to a steady natural stream, it is necessary to subdivide a study reach into a set of steady uniform channels. A river system is visualized first as a flow system consisting of a fixed number of stream tubes with equal subdischarge Δq. This is shown in figure 31. Note that all solid lines represent impervious boundaries through which no convection and diffusion take place. The system is then divided into a set of subreaches depending on the uniformity of cross-sectional properties. A subreach may further be divided into subchannels depending on the location of tributaries and islands as illustrated in figure 31. In the stream-tube flow system longitudinal distance remains the same as in the real river system.

Solutions to "conservative" excess temperature, T'_e, are obtained for successive downstream subreaches starting at the waste heat discharge site. For each uniform subchannel, an upstream T'_e is treated as the initial temperature, T_{eo}, and downstream T'_e is calculated by means of equation 48. In most applications, the upstream temperature tends to be different from one stream tube to another so that a superposition of solutions is required to obtain the downstream T'_e resulting from all upstream temperatures. This procedure is justified because all differential equations involved are linear equations.

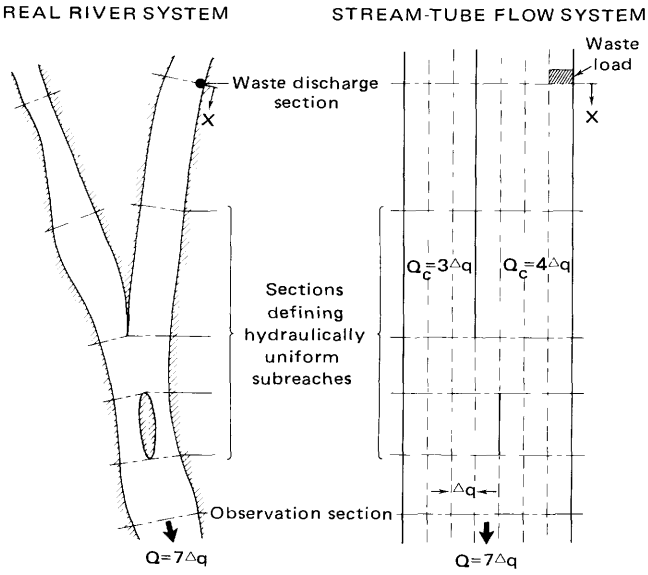

FIGURE 31.—Sketch of a two-dimensional natural stream and its stream-tube flow system.

Once the steady-state T'_e is found for the entire reach, the calculation of exponential decay is initiated by choosing a set of times, t, at which excess temperature is desired at a downstream cross section. The travel time, τ, between the discharge site and the desired cross section and the initial time, t_o, are then determined, and the exponential loss factor is calculated, as in the one-dimensional model. The cross-sectional loss factor thus obtained is applied to T'_e according to equation 45 to obtain actual excess temperature $T_e(t)$ at various longitudinal and transverse positions. This may be added to natural temperature, T_n, to obtain actual temperature T. In field problems, the excess temperature at a discharge site tends to vary with time even if waste water discharge rates remain steady. This time variation in excess temperature at the discharge site may be accounted for in Lagrangian decay calculations for field applications.

As stated previously, the above model is not proposed as an exact solution to a boundary value problem but as an adequate simulation of physical phenomena without burdening oneself with time-consuming numerical solutions to the original set of equations. The validity of this approach can be assessed by comparing the model calculations with observed data.

APPLICATIONS TO FIELD DATA

Temperature regimes observed near Dickerson Power plant on the Potomac River were ideal for testing the two-dimensional model. Figure 3 gives a sketch of the study reach. The surveys conducted in March and May 1969 showed that the heat plume did not reach the right bank for a downstream distance of 35 km and the transverse variation of excess temperature was quite pronounced throughout the study reach. In the November study, on the other hand, the heated effluent discharge was 36 percent of the total discharge and the heat plume was observed to reach the right bank at about 1.3 km downstream. A tremendous increase in effective transverse mixing was caused by density stratification, jet effect of effluent water as well as low stream velocity.

One of the major tasks in the analysis was to assess the magnitude of dispersion coefficient, $\{K_z\}$, to be used in thermal diffusion. Two dye tracer studies conducted at the time of the March survey turned out to be useful in this connection. The first study was for the purpose of determining the traveltime in the left channel (3.64 km long) along Mason Island using 2 kg of rhodamine WT dye, which was injected as an instantaneous line source. The observed dye velocity was 0.46 $m \cdot sec^{-1}$ and about 10 percent smaller than 0.51 $m \cdot sec^{-1}$ estimated from gaging data at sections 4, 5, and 6.

The purpose of the second dye study was to tag heated water from the power plant. A rhodamine WT 20 percent solution was continuously injected at a rate of 4.2 $g \cdot sec^{-1}$ into an upstream area of the effluent canal for about 5.5 hours. The mixing in the canal was intense enough to produce a uniform concentration of 11.2 micrograms per liter in the canal at its outlet (section 2) to the Potomac River. Figure 32 shows transverse distributions of both WT dye concentration and T_e, which were concurrently observed at several downstream sections. Both coordinates are nondimensionalized by arbitrary scales for easier comparison. Good overall agreement between the diffusion of dye and excess temperature is indicated in figure 32. When the dye data were compared with T_e observed at other times, it was found that such T_e's were very much influenced by the magnitude of time-dependent initial excess temperature as well as natural temperature. Therefore, the initial assessment of the dispersion coefficient was based solely on the distribution of rhodamine WT concentration.

For the simulation of March data, the reach between the discharge site (section 2) and White's Ferry site (section 7) was divided into six subreaches, of which the middle three subreaches had two subchannels separated by Mason Island. The total discharge, $Q=148.5$ m^3sec^{-1}, was divided into 48 stream tubes with $\Delta q=3.09$ m^3sec^{-1}. At the effluent site, 4 tubes on the left bank side were taken to be uniformly contaminated by dye and excess heat ($Q_s=12.36$ m^3sec^{-1}). After several trial calculations by equation 48, an optimal value for the transverse dispersion coefficient was found to be

$$\{K_z\}=0.52\{Y\}\{V_*\}, \quad (50)$$

where $\{V_*\}$ is the average shear velocity. The constant 0.52 is larger than 0.08~0.26, a range commonly accepted in straight laboratory flumes and small channels (Prych, 1970; Fischer, 1973) but is close to 0.72 for the Columbia River (Glover, 1964) or 0.6 for the Missouri River (Yotsukura and others, 1970). For a slowly meandering stream such as the Potomac, the constant of 0.52 is a reasonable value. Table 2 contains some hydraulic properties related to the dispersion coefficient.

The calculation of the heat decay was discussed in detail in the previous sections and is not repeated here. Table 2 contains some hydraulic properties related to traveltime, τ, and figure 33 shows the variation of surface dissipation coefficient, U_*, and initial excess temperature T_{eo} with time. In calculating U_*, two sets of meteorologic data obtained at section 4 and section 7 were averaged, because the difference in U_* by the use of individual set was insignificant. Natural temperature observed near the left bank of section 1 was used as T_b in equation 25. The mass transfer coefficient of evaporation, N, was fixed at $1.9\cdot10^{-8}$ kg·m^{-1}·newton^{-1}. As the reach was short and the heat loss was small in the March study, no intensive effort was made to assess the sensitivity of the calculations to the mass transfer coefficient.

TABLE 2.—*Cross-sectional average hydraulic parameters, the Potomac River below Dickerson Power Plant, Maryland, March 1969*

x (in m)	$[v_x]$ (in m·sec^{-1})	$[Y]$ (in m)	$[v_xY^2]$ (in m^3·sec^{-1})	$[V_*]$ (in m·sec^{-1})	$[K_z]$ (in m^2 sec^{-1})	$\Delta x/[v_x]$ (in hours)
2424	0.365	1.07	0.724	0.040	0.0223	1.84
5197	0.58	0.73	0.345	0.033	0.0125	1.33
6061	0.29	1.34	0.765	0.044	0.0304	0.83
7637	0.30	1.74	1.127	0.051	0.0458	1.46

In the March study, the effect of transverse stratification was not observed even at the first survey section, section 3, which was 1.3 km downstream from the discharge site. The effluent canal joins the Potomac River at an angle less than 12°, and velocity in the canal was about the same as that of the Potomac in the March survey. Therefore, the jet effect of effluent discharge was absent. Large transverse temperature gradients and, thus, density gradients near the discharge site must have caused transverse mixing much more intense than that due to turbulence alone. The effect

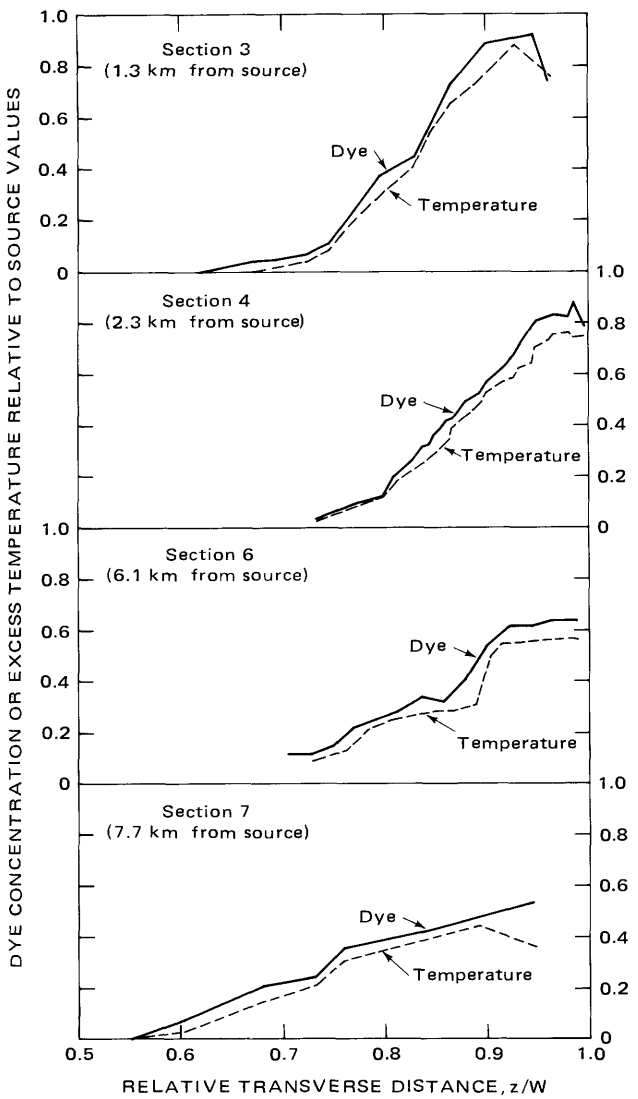

FIGURE 32.—Concurrent transverse distributions of dye concentration and excess temperature, the Potomac River below Dickerson Power Plant, Maryland, 1969.

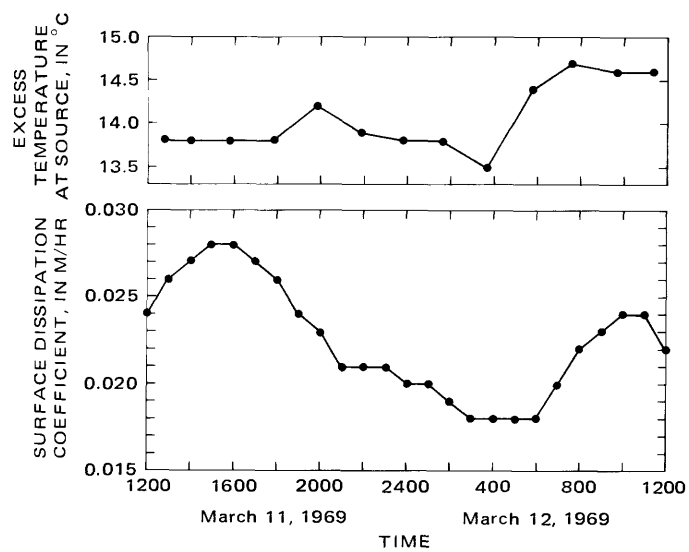

FIGURE 33.—Temporal variations of surface heat dissipation coefficient and source excess temperature, the Potomac River below Dickerson Power Plant, Maryland, March 1969.

apparently was limited to a region very close to section 2 and could not be detected at section 3, where the ration, $x/\{Y\}$, was on the order of 1300.

The calculated T_e was added to T_n which was obtained by the one-dimensional analysis using equation 39. The calculated temperature, T, is plotted against transverse position expressed by cumulative discharge, q', at sections 3, 4 and 7 at selected times in figure 34. Also plotted on these figures are the observed temperatures. The agreement between the predicted and observed temperature is satisfactory. One obvious reason is that the total heat loss through the air-water interface was small, amounting to only 10 percent of the initial excess heat at section 7, the furthest station. Thus, the transverse distribution was determined predominantly by diffusion. Another reason for good agreement is that high wind speed and, thus, high values of U_* induced rather uniform dissipation in the transverse direction, as assumed in the model. Some of the discrepancies between the observed and calculated temperatures are believed to be due to the transverse variation of T_n, which is not accounted for in the model. As mentioned earlier, the data at section 1 showed that such variations amounted to 1°C occasionally.

Analysis of the May data was more involved than the March data, because the length of the study reach

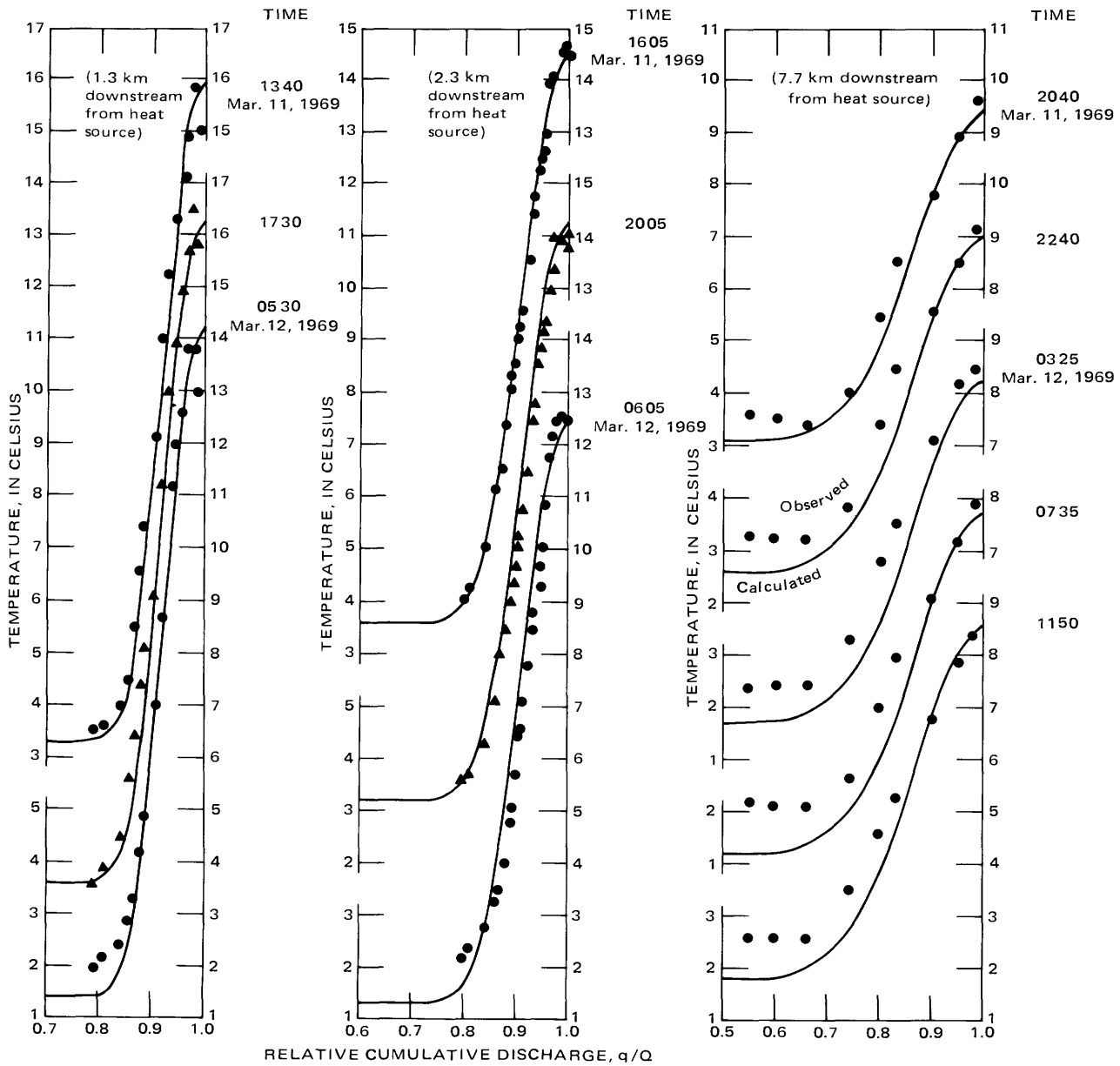

FIGURE 34.—Comparison of observed and calculated transverse temperature distributions, the Potomac River below Dickerson Power Plant, Maryland, March 1969.

was extended to 29 km to cover the Seneca area. One major problem with the May data was to extrapolate meteorologic and thermal-effluent source data for about 1½ days prior to the start of the actual thermal-survey period, May 14–15, 1969. This was necessary for Lagrangian heat-decay calculations, because the average travel time of a packet of water from the plant site to Seneca was 29.8 hours. The water, whose temperature was observed at Seneca at 1300 hours, May 14, had left the plant site at 0710 hours, May 13, and had been undergoing surface heat exchange for an appreciable period of time, which was not covered by the 24 hour survey starting at 1200 hours, May 14.

The extrapolation of T_s and T_n data was accomplished by use of the temperature record kept by the Dickerson Power Plant for the condenser units No. 2 and 3. The extrapolation of T_s was relatively easy, because T_s observed at the effluent canal was very close to an average of exit temperatures recorded at units 2 and 3 at the corresponding time. On the other hand, intake temperatures recorded at condenser units 2 and 3 indicated some stratification effects, because they were about 2°C lower than the observed natural temperature in the Potomac at section 1. The extrapolations of T_n and $T_{eo}=T_s-T_n$ were not very satisfactory, probably containing an error of ±1.5°C.

The meteorologic data were extrapolated by comparing observed data at the river site with those recorded at the National Weather Service Station at Dulles International Airport, Virginia, which is about 40 km west of the study site. Partly because of this need for extrapolation, the two sets of meteorologic data obtained at sections 2 and 9 were again averaged to produce a single time-series set to be used for the entire reach. The averaging and extrapolation is believed to have a relatively small effect on the values of U_*.

The river discharges in May were only 10 percent less than that in the March survey period. It was expected that diffusion factors would remain similar for the subreaches between sections 2 and 7. After several trials, it was decided that the transverse diffusion factors for the May regime be kept the same as for the March regime (table 2). Taking account of observed local depth and velocity, this amounted to using the constant in equation 50 ranging from 0.56 for section 3 to 0.65 for section 7. A constant of 0.65 was used for the lower subreaches that included sections 9 and 10. The total discharge, $Q=133.2$ m$^3\cdot$sec^{-1}, was divided into 40 stream tubes, of which 4 tubes near the left bank were assigned for thermal effluents with uniform excess temperature ($Q_s=13.32$ m$^3\cdot$sec^{-1}).

The calculation of surface heat dissipation was based on U_* values shown in figure 35. These values, ranging from 0.009 to 0.018 m$\cdot$hour^{-1}, are much lower than the

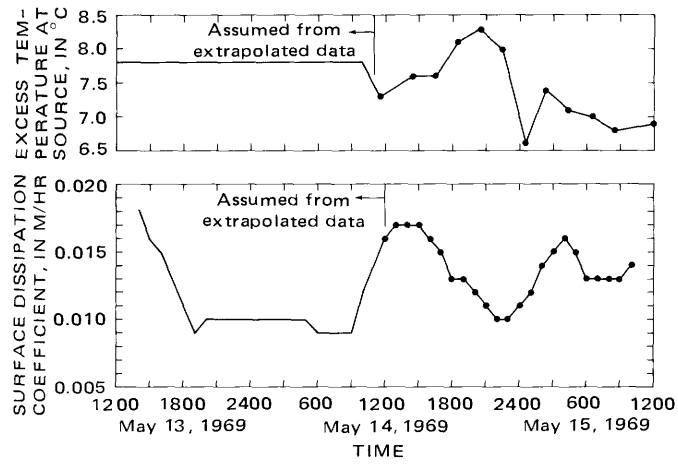

FIGURE 35.—Temporal variations of surface heat dissipation coefficient and source excess temperature, the Potomac River below Dickerson Power Plant, Maryland, May 1969.

March values and are obviously due to lower wind speed in the May period.

The calculated temperature, T, is compared with the observed temperature in figures 36 and 37 in the manner similar to figure 34. Despite large amounts of extrapolated input data, the agreement in temperature distributions at sections 4, 9, and 10 are satisfactory. Some discrepancies observed at sections 4 and 9 may be attributed to either local weather conditions, which were not represented in the U_* values, or T_n variations in the transverse direction. These discrepancies are observed late at night or early in the morning. The calculated T_e at Seneca, section 10, shows that the heated plume, $T_e\geq 0.05$°C, occupies 70 percent of total discharge, leaving 30 percent of the discharge near the right bank uncontaminated. According to the calculations, the total heat loss at Seneca is only 25 percent of the initial excess heat after 29.8 hours of travel from the discharge site.

The results at White's Ferry, section 7, are not very satisfactory. The calculations overestimate left bank temperature and underestimate midstream temperature between $q/Q=0.55$ and 0.75. The peculiar midstream distribution with a hump is not due to turbulent diffusion, which dictates a smoother transverse distribution. A more likely cause is either transverse variation of T_n or local transverse convection by secondary flows. Since the March and October data do not show such a pronounced hump, the effect of secondary flow is likely to be less than that of T_n variation. On the other hand, the variation of T_n was small in the May data according to observations at section 1. The source of this error at section 7 could not be assessed in further detail.

The October data for the Potomac River illustrate an

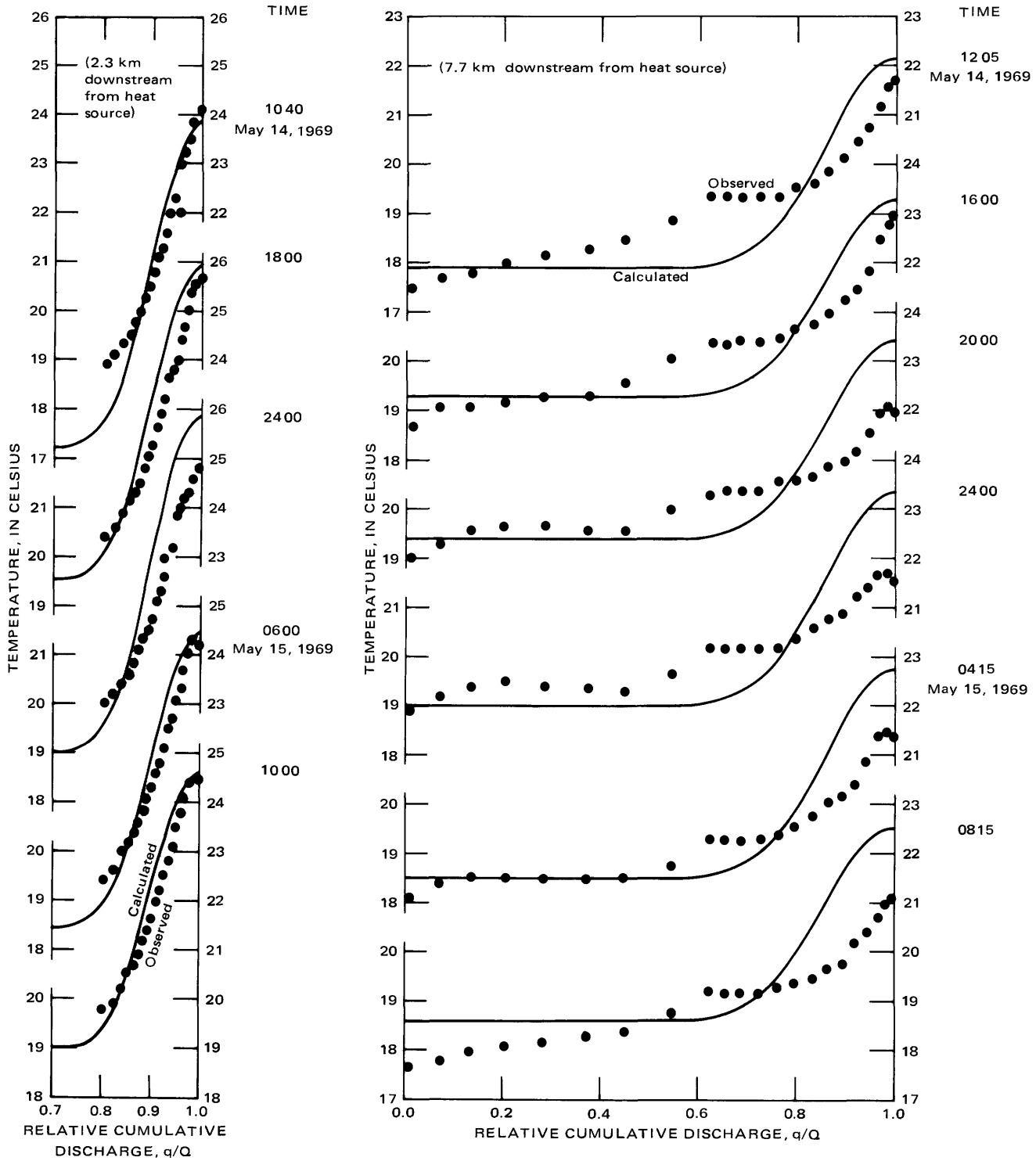

FIGURE 36.—Comparison of observed and calculated transverse temperature distributions, the Potomac River below Dickerson Power plant, Maryland, May 1969.

interesting effect of jet and transverse density currents of heated effluents. The Potomac flow was much lower in October relative to those in March and May. The effluent discharge of 18 $m^3 \cdot sec^{-1}$ was flowing into the ambient Potomac discharge of 32 $m^3 \cdot sec^{-1}$. The ratio, Q_s/Q, was 36 percent. Furthermore, the effluent velocity of 0.90 $m \cdot sec^{-1}$ was high in comparison to the ambient Potomac velocity of 0.2 $m \cdot sec^{-1}$. The combined

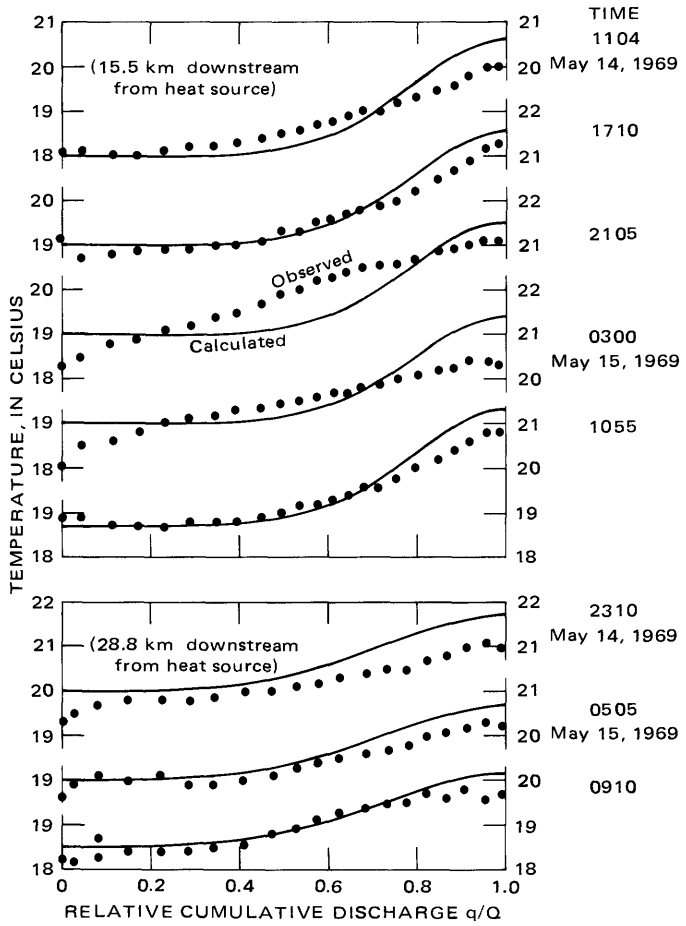

FIGURE 37.—Comparison of observed and calculated transverse temperature distributions, the Potomac River below Dickerson Power Plant, Maryland, May 1969.

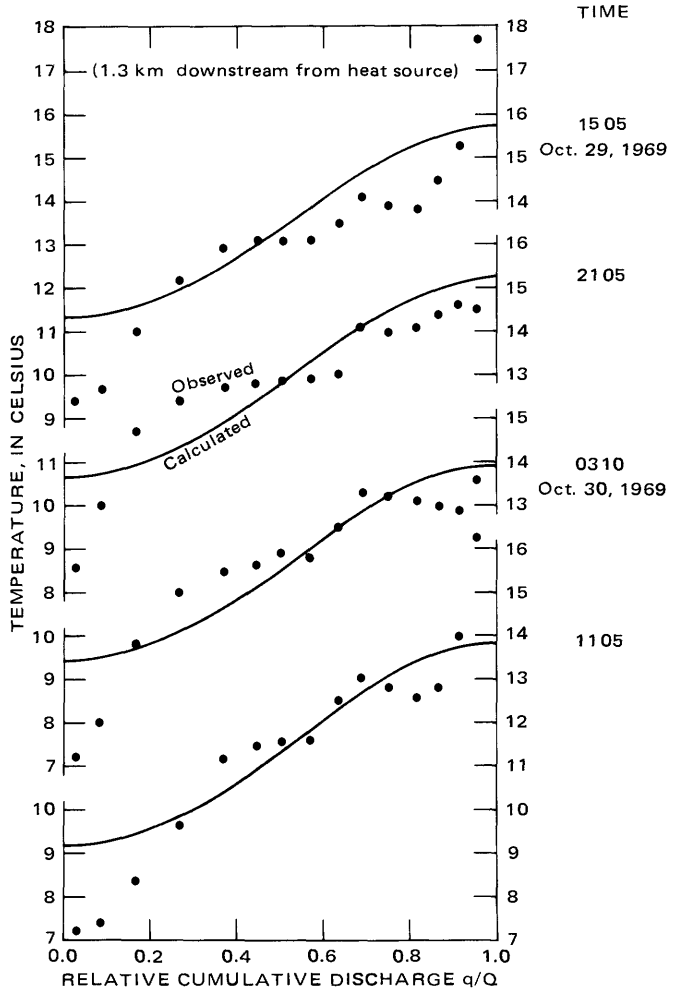

FIGURE 38.—Comparison of observed and calculated transverse temperature distributions, the Potomac River below Dickerson Power Plant, Maryland, October 1969.

effect of jet and transverse convection due to density currents was observable at section 3, where the vertical temperature difference of more than 0.5°C existed between 40 and 20 m from the right bank. The depth in this area was 1.4–2.2 m. The total heated plume width at section 3 was on the order of 200 m in contrast to the width of 70 m in the March study, and the right edge of the plume was characterized by a 20-m-wide band of vertical nonuniformity in temperature.

Even though the present model assumes that the depth-averaged transverse velocity, v_z, is zero everywhere, some transverse convective effects due to secondary flows or density currents are accommodated in the equation in terms of effective dispersion coefficient, K_z. The model can not accommodate the convective effects of jets or very strong secondary currents. An effort was made to simulate the distribution at section 3 by increasing the diffusion factor until the calculation matches with the data. The best simulation is shown in figure 38. In this calculation, the constant of the dispersion coefficient, equation 50, was increased to 11.0 from 0.52. On the other hand, a constant of 0.65 could be used in all other downstream sections as expected. The results of calculations for lower subreaches are shown in figures 39 and 40.

In the October study as in the May study, meteorologic and effluent temperature data were extrapolated by comparing the survey data with those recorded at Dickerson Power Plant and Dulles weather station. Because the travel time to a downstream section was much longer than that for the May study, being 11.2, 25.7, and 59.7 hours for sections 7, 9, and 10 respectively, almost half of the calculations for section 7 and all calculations for section 9 used some parts of extrapolated data. The calculation at section 10 was not tried. The heat dissipation coefficient, U_*, varied from 0.007 to 0.02 m·hour^{-1}. This range is rather similar to that of the May study, indicating the predominant effect of wind speed on U_*. The simulation results shown in figures 38, 39, and 40 show that the present model

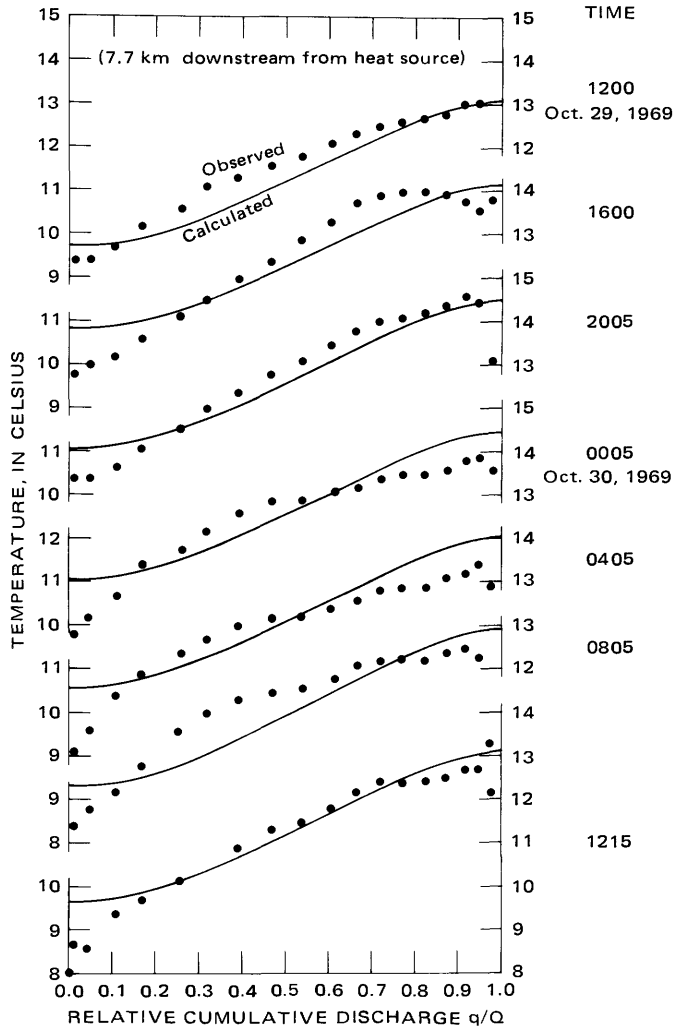

FIGURE 39.—Comparison of observed and calculated transverse temperature distributions, the Potomac River below Dickerson Power Plant, Maryland, October 19

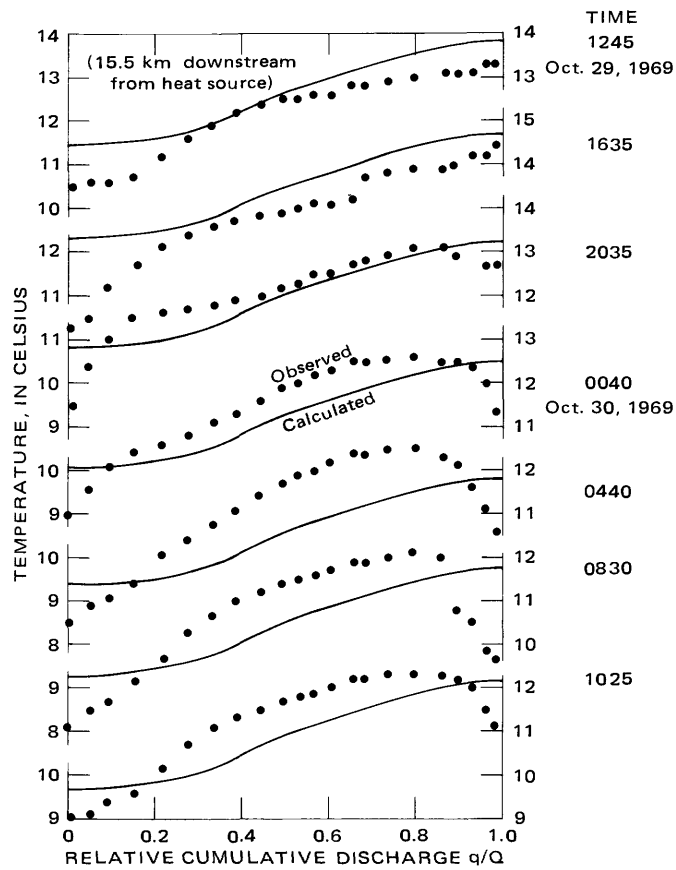

FIGURE 40.—Comparison observed and calculated transverse temperature distributions, the Potomac River below Dickerson Power Plant, Maryland, October 1969.

with more adequate weather data and with current knowledge on dispersion coefficient can predict heated plume configurations with acceptable accuracy.

As for the effects of transverse density currents, it is worth mentioning the results of flume study reported by Prych (1970). He studied the transverse diffusion of excess heat in a rectangular flume by releasing a vertical line heat source at ambient velocity. It is reported that the total transverse variance, σ_a^2, could be considered as a sum of σ_t^2 due to regular turbulence diffusivity and σ_s^2 due to density currents. At a distance on the order of $x/\{Y\}=2\{v_x\}\{Y\}/\{K_z\}$, σ_s^2 stopped increasing because of reduced density currents, and the increase of σ_a^2 thereafter was entirely due to σ_t^2.

The prototype distance x corresponding to Prych's criterion is on the order of 30–50 m for the October data and is much smaller than $x=1330$ m at section 3. Because the heat source on the Potomac River was a block source rather than the line source used in the Prych's study, the effect of density currents must have persisted for a much longer distance than 30 or 50 m. Similar effects must have been existent in the March and May data but were not observed at section 3. The observed pattern of density effects appears to agree with Prych's laboratory study.

The two-dimensional model was also applied to the Dan River and the North Platte River data. In both rivers the transverse nonuniformity of excess temperature was significant only in one downstream subreach. Because the river alinement was quite sinuous in both rivers, the temperature distributions at other subreaches were all uniform in the transverse direction. The one-dimensional analysis of these subreaches was discussed previously. Figures 41 and 42 present the simulations for one subreach in the Dan River and the North Platte River, respectively. The heat decay in these calculations was insignificant because the subreach length was small. The observed temperature distribution at the first cross section was used as the initial distribution in the calculation, because the effluent discharge condition was not compatible with the

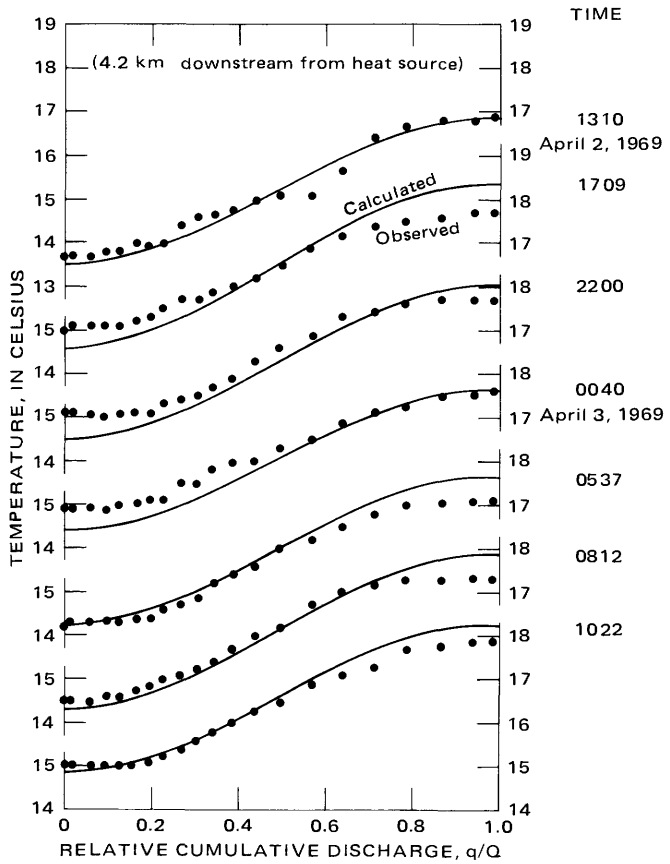

FIGURE 41.—Comparison of observed and calculated transverse temperature distributions, the Dan River near Eden, North Carolina, April 1969.

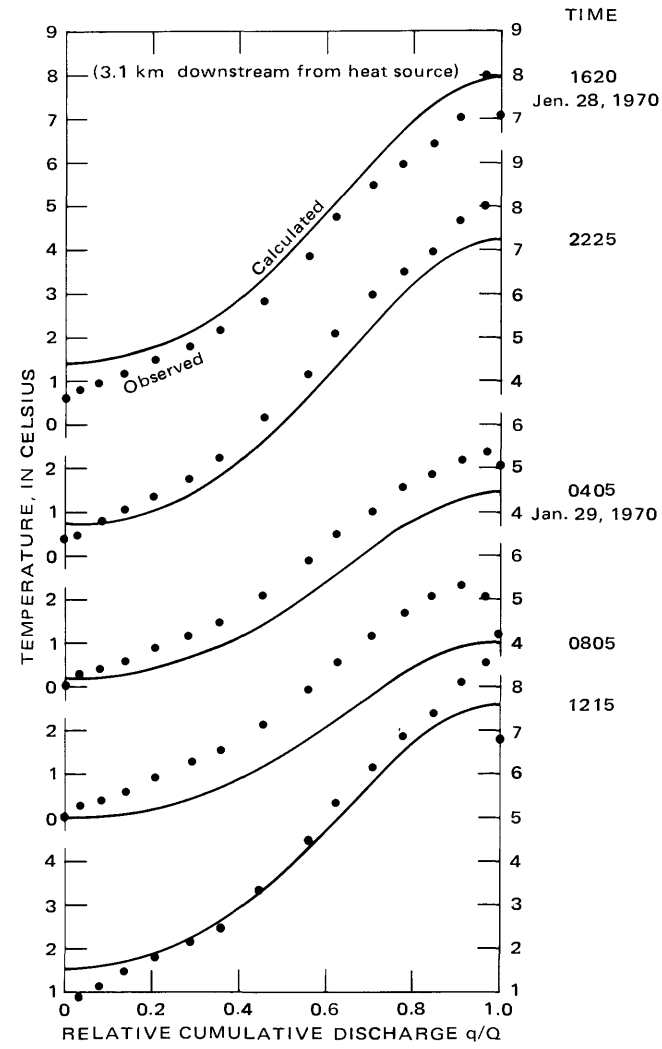

FIGURE 42.—Comparison of observed and calculated transverse temperature distributions, the North Platte River near Glenrock, Wyoming, January 1970.

model. Because of these reasons, figures 41 and 42 are considered as verifying the diffusion aspect of the model. A constant of 0.65 in equation 50 was used for both simulations.

SUMMARY REGARDING TWO-DIMENSIONAL MODEL

Ideally, a two-dimensional model for excess temperature should be combined with a two-dimensional model for natural temperature. The latter model was not developed in the present analysis, and thus some discrepancies between observed and calculated temperatures could not be resolved for the assessment of the two-dimensional model. A typical example is the low temperature near the banks as observed in figure 40.

Nevertheless, the overall performance of the present model appears to confirm that the combination of the steady-state diffusion solution and the Lagrangian decay solution is a feasible approach. In this connection, it is worth noting that an attempt was made in the early stage of analysis to solve equation 43 directly by Eulerian numerical approximations. It was abandoned because the calculations were much more time consuming and inefficient in terms of solution accuracies than the above-discussed model.

A substantial amount of data extrapolation was required for the two-dimensional analysis. This was caused by the incompatibility between the data collection scheme and the model development as noted previously. If thermal data are collected for the purpose of applying the present Lagrangian model, it is clear that the reach length and the travel time should be of prime considerations in planning such a data collection scheme.

It is apparent that verification concerning the transport phase is more positive than that for the decay phase. A comparison of the present findings with other studies shows that there is little doubt that the transverse heat dispersion coefficient, K_z, in the absence of abrupt temperature changes, is of the same order of magnitude as the mass dispersion coefficient for neutrally buoyant solutes. Even though the formulation of

equation 42 assumes no depth-averaged transverse velocity, the weak convective effect due to secondary or density currents is accommodated in terms of dispersion coefficient, K_z. Furthermore, by means of empirical adjustment of K_z, some pronounced convective effects could also be simulated by the model as shown in figure 38.

The analysis of the surface-heat decay in the present section is rather limited, as it was evaluated only for the Potomac reach, where heat losses were not significant at most cross sections. Comparing a total heat loss of 25 percent, calculated for the section at Seneca by the two-dimensional model, with an observed value of 35 percent of figure 11, the magnitudes of both the dissipation coefficient, U_*, and the mass-transfer coefficient for evaporation, N, used in the present section may have been too low. The decay aspect has been discussed more extensively in the section on the one-dimensional model of excess temperature.

SUMMARY AND CONCLUSIONS

As explained in the "Introduction," development of the present mathematical models was based on the recognition that earlier models, such as the energy-budget equation, the equilibrium temperature, and the steady-state exponential decay law, are not suitable in analyzing short-term phenomena in a flowing natural stream. In concluding the report, therefore, it is appropriate to summarize pertinent features of the present mathematical models.

In order to approach short-term water temperature problems in a thermally loaded stream, the excess temperature, T_e, is defined as a difference between actual water temperature, T, and natural temperature, T_n, which would exist in the stream under the same hydraulic and meteorologic conditions but without heat discharges. One major feature of the present approach is to solve the heat conservation equation separately for T_e and T_n. Both temperatures are functions of time and space variables.

Starting from a three-dimensional equation for conservation of thermal energy in a turbulent flow, two- and one-dimensional equations for water temperature, T, are obtained by integrating the equation, first, with respect to depth and, second, with respect to surface width of a stream channel. Two assumptions involved are that the heat exchange between water and surrounding media takes place at the interface without storage and that the introduction of dispersion coefficients is justified empirically. No formal assumptions are required as to the steadiness or uniformity of a flow as long as the gradient-type dispersion terms are acceptable approximations.

The equation for T_e is obtained by subtracting the equation for T_n from that for T. Assuming that the entire heat exchange occurs at the air-water interface, the resulting equation is shown to be independent of incoming solar and atmospheric radiation fluxes, the measurement of which requires expensive instrumentation. Three other essential heat fluxes, namely, back radiation, latent heat of evaporation, and conduction are dependent on transient meteorologic conditions and are nonlinear functions of water temperature. However, these fluxes can be linearized with respect to T, provided that an arbitrarily chosen base temperature of linearization, T_b, does not deviate excessively from both T and T_n. The surface heat dissipation coefficient, U, is simply the sum of the first derivatives of the three heat fluxes with respect to temperature evaluated at T_b. In this manner, the equation for T_e is reduced to a linear equation.

The one-dimensional equation for T_e may be further reduced to an ordinary differential equation by neglecting the longitudinal dispersion term and adopting the Lagrangian approach, which employs mean traveltime as the only independent variable. If time-varying initial excess temperature and wind speed are given as inputs, the excess temperature can be solved as a function of traveltime. For the two-dimensional equation for T_e, a steady-state Eulerian solution is obtained for a hypothetical "conservative" excess temperature, assuming that both stream and waste heat discharges remain steady. The actual excess temperature is approximated by multiplying the "conservative" excess temperature by the Lagrangian heat decay factor similar to the one-dimensional model.

Only a one-dimensional model is considered for natural temperature in this analysis. The incoming solar and atmospheric radiations are important input data. Linearization of the other three heat fluxes is not employed in the equation for T_n, because the nonlinear effect is small in the normal range of variation of T_n and these three fluxes at certain times are adequately approximated by use of the known temperature at an immediately preceding time. The solutions are obtained by use of the Lagrangian method. A simpler method based on the "thermally homogeneous stream" assumes that T_n is a function of time alone everywhere in a stream. The method has an advantage of requiring lesser amounts of input data than the Lagrangian method.

The second part of the report is devoted to the detailed analysis of data by the mathematical models. A summary of the result is given at the end of the sections describing, respectively, one-dimensional natural temperature, one-dimensional excess temperature, and two-dimensional excess temperature. Several con-

clusions may be drawn from the analysis.

The one- and two-dimensional models presented in this report provide adequate descriptions for the variation of natural as well as thermally loaded temperatures in a natural stream reach on the order of 30 km in length. There were some streams in which large discrepancies were noticed between observed and calculated temperatures. In some cases these errors can be traced to large amounts of ground-water accretion and longitudinal dispersion, both of which are neglected in the model. The majority of errors, however, can be attributed to inadequate input data, as well as uncertainty about the mass-transfer coefficient of evaporation.

The transport aspects of the present models are generally satisfactory. Longitudinal dispersion terms may safely be neglected in temperature equations even under a typical diurnal cycle of waste heat discharges such as seen below power plants. Optimum values for the transverse dispersion coefficient of heat were found to be 0.52 to $0.65 \cdot \{Y\} \cdot \{V_*\}$, corresponding to the range commonly accepted for solute masses. As indicated by the Potomac River data, transverse mixing is a very slow process for diluting excess heat.

As for surface heat dissipation aspects, the one-dimensional excess temperature model clearly indicates the dominant effect of the wind speed and the mass-transfer coefficient of evaporation. An optimum value for the latter was $2.7 \cdot 10^{-8}$ $kg \cdot m^{-1} \cdot newton^{-1}$. Further stream studies on forced evaporation are desirable, especially under unstable atmospheric conditions. No definite conclusions could be obtained from the tests of the one-dimensional natural temperature model and the two-dimensional excess temperature model with regard to the mass-transfer coefficient.

The data as well as the analysis of excess temperature strongly indicate that heat dissipation through the air-water interface is also a very slow natural process in removing excess heat. No more than 50 percent of initial excess heat was dissipated in reaches of most streams under investigation. Therefore, this aspect should be given an adequate consideration in planning or regulating operations of a series of power plants along a river system.

REFERENCES CITED

Anderson, E. R., 1954, Energy-budget studies, water-loss investigations, Lake Hefner studies, Technical Report: U.S. Geol. Survey Prof, Paper 269, p. 71–119.

Bowen, I. S., 1926, The ratio of heat losses by conduction and by evaporation from any water surface: Phys. Rev., Ser. 2, v. 27, p. 779–787.

Brown, G. W., 1972, An improved temperature prediction model for small streams: Water Resources Research Inst. Report WRRI–16, Oregon State Univ., Corvallis, Oregon, 20 .

Brutsaert, W., and Yeh, G. T., 1970, Implications of a type of empirical evaporation formula for lakes and pans: Water Resources Research, v. 6, no 4, p. 1202–1208.

Crank, J., 1967, The mathematics of diffusion: London, Oxford University Press, p. 120–132.

Edinger, J. E., and Geyer, J. C., 1965, Heat exchange in the environment: EEI Publ. No. 65–902, Edison Electric Inst., New York, 259 p.

Ewing, G., and McAlister, E. D., 1960, On the thermal boundary layer of the ocean: Science, v. 131, p. 1374–1376.

Fischer, H. B., 1973, Longitudinal dispersion and turbulent mixing in open channel flow, *in* Annual Review of Fluid Mechanics, v. 5: Palo Alto, Calif., Annual Reviews Inc., p. 59–78.

Glover, R. E., 1964, Dispersion of dissolved or suspended materials in flowing streams: U.S. Geol. Survey Prof. Paper 433–B, 32 p.

Harbeck, G. E., Jr., 1953, The use of reservoirs and lakes for the dissipation of heat: U.S. Geol. Survey Circ. 282, 6 p.

———1962, A practical field technique for measuring reservoir evaporation utilizing mass-transfer theory: U.S. Geol. Survey Prof. Paper 272–E, p. 101–105.

———1970, Discussion on the cooling of riverside thermal-power plants, in Parker, F. L. and Krenkel, P. A., eds., Engineering Aspects of Thermal Pollution: Nashville, Tenn., Vanderbilt Univ. Press, p. 133–143.

Harbeck, G. E., Jr., Koberg, G. E., and Hughes, G. H., 1959, The effect of the addition of heat from a power plant on the thermal structure and evaporation of Lake Colorado City, Texas: U.S. Geol. Survey Prof. Paper 272–B, 49 p.

Harbeck, G. E., Jr., Kohler, M. A., Koberg, G. E., and others, 1958, Water-loss investigations, Lake Mead studies: U.S. Geol. Survey Prof. Paper 298, 100 p.

Harbeck, G. E., Jr., Meyers, J. S., and Hughes, G. H., 1966, Effect of an increased heat load on the thermal structure and evaporation of Lake Colorado City, Texas: Texas Water Development Board report 24.

Harleman, D. R. F., 1972, Longitudinal temperature distribution in rivers and estuaries, one-dimensional mathematical models: Engineering Aspects of Heat Disposal from Power Generation, MIT Summer Session, Cambridge, Mass.

Hinze, J. O., 1959, Turbulence: New York, McGraw-Hill Book Co., 586 p.

Holley, E. R., 1971, Transverse mixing in rivers: Delft Hydraulics Lab. Rept. S132, Delft, The Netherlands, 92 p.

Jackman, A. P., and Meyer, E. L., 1971, Basic data on heat dissipation downstream from large heat sources: Health Physics. Soc., 5th Ann. Midyear Mtg., a symposium, 8 p.

Jaske, R. T., 1969, Thermal modification of river quality: Rept. BNWL–719, Pacific Northwest Lab., Richland, Wash., 6 p.

Jobson, H. E., 1972, Effect of using averaged data on the computed evaporation: Water Resources Research, v. 8, no. 2, p. 513–518.

———1973a, The dissipation of excess heat from water systems: Am. Soc. Civil Engineers, Jour. Power Div., v. 99, no. PO1, p. 89–103.

———1973b, Evaluation of turbulent transfer laws used in computing evaporation rates: U.S. Geol. Survey open-file report, 169 p.

Jobson, H. E., and Yotsukura, N., 1973, Mechanics of heat transfer in nonstratified open-channel flows, *in* Shen, H. W., Environmental Impact on Rivers: For Collins, Colo. p. 8.1–8.67.

Koberg, G. E., 1964, Methods to compute long-wave radiation from the atmosphere and reflected solar radiation from a water surface: U.S. Geol. Survey Prof. Paper 272–F, p. 107–136.

Leendertse, J. J., 1970, A water-quality simulation model for well-mixed estuaries and coastal seas; Vol. 1, Principles of Computation: Santa Monica, Calif., Rand Corp. Memo. RM–6230–RC.

McAlister, E. D., and McLeish, W., 1969, Heat transfer in the top

millimeter of the ocean: Jour. Geophys. Research, v. 74, no. 13, p. 3408–3414.

Marciano, J. J., and Harbeck, G. E., Jr., 1954, Mass-transfer studies, water-loss investigations, Lake Hefner studies, Technical Report: U.S. Geol. Survey Prof. Paper 269, p. 46–70.

Messinger, H., 1963, Dissipation of heat from a thermally loaded stream: U.S. Geol. Survey Prof. Paper 475–C, p. C175–C178.

Morse, W. L., 1970, Stream temperature prediction model: Water Resources Research, v. 6, no. 1, p. 290–302.

Pai, S. I., 1956, Viscous flow theory, I-laminar flow: Princeton, N.J., D. Van Nostrand Co., Inc., p. 41–43.

Parker, F. L., and Krenkel, P. A., 1969, Engineering aspects of thermal pollution: Nashville, Tenn., Vanderbilt Univ. Press, 351 p.

Pierson, F. W., and Jackman, A. P., 1975, An investigation of the predictive ability of several evaporation equations: Jour. Appl. Meteorology, v. 14, no. 4, p. 477–487.

Pluhowski, E. J., 1970, Urbanization and its effect on the temperature of the streams on Long Island, New York: U.S. Geol. Survey Prof. Paper 627–D, 110 p.

Priestly, C. H. B., 1959, Turbulent transfer in the lower atmosphere: Chicago, Ill., Univ. Chicago Press.

Prych, E. A., 1970, Effect of density difference in lateral mixing in open-channel flows: Rept. no. KH–R–21, Pasadena, Calif., Calif. Inst. Tech., 225 p.

Sayre, W. W., 1973, Natural mixing processes in rivers, *in* Shen, H. W., ed., Environmental Impact on Rivers: Fort Collins, Colo., p. 6.1–6.37.

Sellers, W. D., 1965, Physical climatology: Chicago, Ill., Univ. Chicago Press, 272 p.

Taylor, G. I., 1954, The dispersion of matter in turbulent flow through a pipe: Proc. Royal Soc., London, v. 223 A, p. 446–468.

Thomann, R. V., 1973, Effect of longitudinal dispersion on dynamic water quality response of streams and rivers: Water Resources Research, v. 9, no. 2, p. 355–366.

Yeh, G. T., Verma, A. P., and Lai, F. H., 1973, Unsteady temperature prediction for cooling ponds: Water Resources Research, v. 9, no. 6, p. 1555–1563.

Yotsukura, N., 1972, A two-dimensional temperature model for a thermally loaded river with steady discharge: Contribution to the 11th Ann. Environmental and Water Resources Eng. Conf., Vanderbilt Univ., Nashville, Tenn., p. 13–26.

Yotsukura, N., and Cobb, E. D., 1972, Transverse diffusion of solutes in natural streams: U.S. Geol. Survey Prof. Paper 582–C, 19 p.

Yotsukura, N., Fischer, H. B., and Sayre, W. W., 1970, Measurement of mixing characteristics of the Missouri River between Sioux City, Iowa, and Plattsmouth, Nebraska: U.S. Geol. Survey Water Supply Paper 1899–G, 29 p.

Yotsukura, N., Jackman, A. P., and Faust, C. R., 1973, Approximation of heat exchange at the air-water interface: Water Resources Research, v. 9, no. 1, p. 118–128.

☆U.S. GOVERNMENT PRINTING OFFICE: 1977 - 789-025/50